Monkeypox Virus: The Battle between Necroptosis Inhibition and the Antiviral Innate Response

by

Jacqueline Krystal Williams

A Dissertation Presented in Partial Fulfillment
of the Requirements for the Degree
Doctor of Philosophy

Approved September 2022 by the
Graduate Supervisory Committee:

Bertram Jacobs, Chair
Jeffrey Langland
Doug Lake
Arvind Varsani

ARIZONA STATE UNIVERSITY

December 2022

ABSTRACT

Monkeypox virus (MPXV) is an orthopoxvirus that causes smallpox-like disease and has up to a 10% mortality rate, depending on the infectious strain. The global eradication of the smallpox virus has led to the decrease in smallpox vaccinations, which has led to a drastic increase in the number of human MPXV cases. MPXV has been named the most important orthopoxvirus to infect humans since the eradication of smallpox and has been the causative agent of the 2022 world-wide MPXV outbreak. Despite being highly pathogenic, MPXV contains a natural truncation at the N-terminus of its E3 homologue. Vaccinia virus (VACV) E3 protein has two domains: an N-terminus Z-form nucleic acid binding domain (Z-BD) and a C-terminus double stranded RNA binding domain (dsRBD). Both domains are required for pathogenesis, interferon (IFN) resistance, and protein kinase R (PKR) inhibition. The N-terminus is required for evasion of Z-DNA binding protein 1 (ZBP1)-dependent necroptosis. ZBP1 binding to Z-form deoxyribonucleic acid/ribonucleic acid (Z-DNA/RNA) leads to activation of receptor-interacting protein kinase 3 (RIPK3) leading to mixed lineage kinase domain-like (MLKL) phosphorylation, aggregation and cell death. This study investigated how different cell lines combat MPXV infection and how MPXV has evolved ways to circumvent the host response. MPXV is shown to inhibit necroptosis in L929 cells by degrading RIPK3 through the viral inducer of RIPK3 degradation (vIRD) and by inhibiting MLKL aggregation. Additionally, the data shows that IFN treatment efficiently inhibits MPXV replication in a ZBP1-, RIPK3-, and MLKL- dependent manner, but independent of necroptosis. Also, the data suggests that an IFN inducer with a pancaspase or proteasome inhibitor could potentially be a beneficial treatment against

MPXV infections. Furthermore, it reveals a link between PKR and pathogen-induced necroptosis that has not been previously described.

DEDICATION

To my parents.

Thank you for your constant love and support and for providing a great example of what hard work and dedication can accomplish.

To my husband, Brandon.

Thank you for your unconditional love, encouragement and for always standing by my side. This would not have been possible without your support.

To my boys: Henry and Hunter.

You give me the strength to keep going and not give up. Thank you for always brightening up my day. I love you both.

ACKNOWLEDGMENTS

I would like to give a big thank you to Dr. Bert Jacobs. Thank you for allowing me to join your lab and for all your guidance, patience, and support. You have taught me how to think like a scientist and your enthusiasm for science is contagious. To my committee members, Dr. Jeff Langland, Dr. Doug Lake, and Dr. Arvind Varsani, thank you for your time, suggestions, and questions during my presentations. Your feedback has been a key asset in the completion of my dissertation.

To the Jacobs lab, thank you for everything. To the current lab members, James Bonner, Megan McCaughan, Johanne Gerstel, Clayton Hui, and Allan Yanez, thank you for all your valuable feedback/suggestions during lab meetings, and for your hard work in keeping the lab running smoothly. Thank you, Dr. Karen Kibler, for training me in the BSL3 lab and for our great conversations. A special thanks to Dr. Mateusz Szczerba, you have been a great lab mate and an even better friend. Lastly, thank you to the past lab members, especially Dr. Heather Koehler and Dr. Samantha Cotsmire, whose work started the necroptosis story.

Thank you to all my family for your love and support. To all my cousins for always being there no matter what. Thank you for your patience and understanding when I couldn't be there due to a long experiment, presentation, or just plain tired. Thank you for helping me de-stress and keeping me company in the sauna and ice bath. To my friend in San Francisco, Caroline, thank you for all your encouragement and your support and for telling me not to quit when I was having doubts about myself. To my brother, Jerry, thank you for always being there and for the many hours of conversations, I

couldn’t have asked for a better brother. I would not be here today, without the support of everyone listed here. Thank you.

TABLE OF CONTENTS

Page

LIST OF FIGURES viii

CHAPTER

1 INTRODUCTION 1

2 REGULATION OF NECROPTOSIS AND THE TYPE I INTERFERON RESPONSE BY MONKEYPOX VIRUS 15

Abstract 15

Introduction 17

Materials and Methods 20

Results 25

Discussion 33

Figures 36

References 43

3 NECROPTOSIS INHIBITION BY MONKEYPOX VIRUS AND PKR DEPENDENT NECROPTOSIS 47

Abstract 47

Introduction 49

Materials and Methods 53

Results 56

Discussion 64

Figures 67

References 75

CHAPTER Page

4 DISCUSSION AND FUTURE DIRECTIONS 79

REFERENCES 86

LIST OF FIGURES

Figure		Page
1.1	Poxvirus Sensing Pathways	12
1.2	Type I IFN Response	13
1.3	Activating Necroptosis	14
2.1	MPXV Is IFN Sensitive and Does Not Induce Cell Death	36
2.2	IFN Sensitivity Is Dependent on ZBP1, RIPK3, and MLKL but Not PKR	38
2.3	MPXV vIRD Leads to RIPK3 Cleavage and Necroptosis Inhibition	40
2.4	Caspase and Neddylation Inhibition Leads to Increased IFN Sensitivity and MLKL Membrane Localization, but Does Not Lead to Necroptosis	42
3.1	VACV-E3Δ37N Induces Necroptosis in JC Cells	67
3.2	Low dsRNA Is Not Sufficient to Recover VACV-E3Δ37N Growth	68
3.3	Low dsRNA Rescues VACV-E3Δ37N Cell Viability, but RIPK3 Inhibition Is Also Required For Replication in JC Cells	69
3.4	VACV-E3Δ37N Replication Is Dependent on ZBP1, RIPK3, MLKL and PKR	70
3.5	PKR Is Required for VACV-E3Δ37N-mediated Necroptosis	71
3.6	MPXV Inhibits Necroptosis by Cleaving RIPK3	73

CHAPTER 1

INTRODUCTION

Poxviruses

Poxviruses belong to the *Poxviridae* family and are known to infect a wide range of animals. They are divided into two subfamilies, the *Chordopoxvirinae* (poxviruses of vertebrates) and *Entomopoxvirinae* (poxviruses of insects). The *Chordopoxvirinae* are further divided into nine genera, four of which cause human infection (*Orthopoxvirus, Parapoxvirus, Molluscipoxvirus, Yatapoxvirus*). The most notorious virus in the *Orthopoxvirus* genus is variola virus (VARV), the causative agent to smallpox. The prototype in this genus and the most studied is vaccinia virus (VACV) which was the vaccine used to eradicate smallpox. Monkeypox virus (MPXV) also belongs to this genus and is responsible for the current 2022 world-wide outbreak.

Monkeypox virus

MPXV was discovered in 1958 from infected cynomolgus monkeys that were imported to Copenhagen, Denmark [1]. The first human case was reported in 1970 in a 9-month-old child who had smallpox-like symptoms in the Democratic Republic of the Congo (DRC) [2]. Throughout the 1970s, multiple human MPXV infections were detected throughout Africa. In five Central and Western African countries, 47 cases were reported and 38 cases reported in Zaire, with 9% of the cases suspected to be from human-to-human transmission and 91% from animal contact [3 – 4]. In the 1980s, 404 human monkeypox cases were reported in Africa, but remained low in the 1990s/2000s with sporadic infections [3]. In 2003, the first reported outbreak outside of Africa occurred in the midwestern United States where 47 people contracted MPXV from an ill

pet prairie dog that was housed with infected rodents imported from Africa [5]. From 2018-2021 there were isolated MPXV cases in different countries throughout the world, all with links to African travel. In May 2022, MPXV cases began to be reported in Portugal, Spain, Canada, Belgium, Sweden, Italy, and many more countries around the world. As of August 2022, the CDC reports 49,974 confirmed MPXV cases worldwide and 18,417 cases in the United States. The source of the outbreak is still unknown, but the cases had no known link to endemic areas of Africa, thus raising the question if MPXV has been spreading undetected in local communities, or if MPXV has evolved to become more virulent or increased its transmissibility.

There are two MPXV clades in Africa, known as Clade 2 (Western African, Clade 2a and the current epidemic MPXV, Clade 2b) and Clade 1 (Central African/Congo Basin strains). Clade 2 strains are mainly found in Sierra Leone, Nigeria, Liberia, and Côte d'Ivoire and are less pathogenic and human-to-human transmission occurs less than with the Central strain. The Central African strain is reported in the Congo Basin countries (Cameroon and the DRC) and the mortality rate is ~10%, while the West African Strain is less than 1% [6]. Genetic sequencing revealed a 0.55-0.56% nucleotide difference between the two clades and that they cluster separately on a phylogenic tree. They also share 170 orthologs that are 99.4% identical at the protein level. The difference in virulence between the two strains could be due to differences in the orthologs BR-203 (virulence protein), BR-209 (IL-1β binding protein), and COP-C3L (complement protein) [7 – 8]. All the outbreaks that have occurred outside of Africa have been the West African strain.

MPXV can enter through the oropharynx, nasopharynx, or intradermally and can spread through close contact with lesions, bodily fluids and respiratory droplets of infected people or animals [9]. In the past MPXV has been zoonotic, although the natural host reservoir has not been identified. Symptoms of MPXV infection are similar to a mild form of smallpox, however MPXV infection causes lymphadenopathy. The incubation period is 7-14 days but can be up to 21 days. Onset MPXV symptoms include fever, chills, headache, backache, and fatigue, followed by rash that generally starts on the face and disseminates to other body parts. The rash then develops into pustules that can range from a few to several thousands, followed by scabbing [9 – 10].

Treatment for MPXV infection is usually not required as the symptoms are generally mild and self-limiting. Per the CDC, there is no specific treatment for MPXV infections but there are drugs that were approved for the use against smallpox that may be used as treatment. Tecovirimat (also known as TPOXX or ST-246) is currently the treatment of choice and it works by inhibiting viral release from the infected cell. Brincidofovir and Cidofovir are also approved for the treatment of smallpox, and they work by inhibiting the viral DNA polymerase. Vaccinia immune globulin (VIG) may also be given to people with skin conditions, such as eczema, but data on the effectiveness against MPXV infection is lacking. Lastly, two vaccines are currently available, JYNNEOS, which is a live, replication incompetent VACV, and ACAM2000, a live replication competent VACV [11]. However, with the limited supply of the vaccines and the antipox drugs available, new antiviral therapies specifically against MPXV would be greatly beneficial.

Poxvirus replication

Poxviruses are large, enveloped, brick-shaped DNA viruses with genomes that range between 130-300 kb and replicate entirely in the cytoplasm. Poxviruses can enter the host cell by either direct fusion of the viral membrane to the host plasma membrane at neutral pH or by endocytosis at a low pH [12]. Although, there are no known specific cell receptors for binding, 4 viral attachment proteins have been shown to bind to chondroitin sulfate [13], heparan sulfate [14], [3 – 4], and laminin [17], and they have been implicated in viral binding. A multicomplex of 11 viral proteins form the entry fusion complex (EFC), which is required for viral fusion and for core entry [18-19]. The core contains the RNA polymerase, transcription factors, a capping enzyme, and a poly(A) polymerase that are required for viral transcription and once the core enters the cytoplasm, early viral mRNA is synthesized within minutes [20], which encode proteins for evasion of host defenses and enzymes required for DNA replication [21]. The viral core is then uncoated and this releases the viral DNA into the cytoplasm where it functions as the template for transcription of intermediate and late gene expression [22]. Early, intermediate, and late genes are temporally regulated with 118 early genes expressed before DNA replication, and 93 intermediate and late genes expressed after [22]. Poxviral genomes contain hairpins at the ends of the DNA genome which links the DNA strands into a continuous chain [23 – 24]. DNA replication occurs in viral factories located in the cytoplasm, starts at the hairpin termini, and is catalyzed by the poxviral DNA polymerase and the single-stranded DNA binding protein accessory factor [25 – 27]. Subsequently, intermediate gene expression starts, followed by late gene transcription. During this transcription process, there is no specific termination site on the transcripts causing the RNA polymerase to produce long run-on transcripts. If the

genes are on the opposite strand of the genome, the RNA transcripts can hybridize and form double-stranded RNA (dsRNA) [28 – 29]. Intermediate genes encode primarily late transcription factors, and late genes encode for viral structural proteins, viral enzymes, and assembly factors required for new virion formation [30]. The newly synthesized viral DNA is assembled in viral crescents in the viral factories and forms the immature virion [31], but the mechanism for crescent assembly and membrane wrapping has been controversial [32 – 33]. One recent theory is that poxviruses use the retrograde pathway to transport proteins from endosomes to the *trans*-Golgi network and this is required for membrane wrapping and for viral dissemination [34]. Poxvirus virions can then exit as three distinct infectious forms: mature virions (MV, also known as intracellular mature virus (IMV)), wrapped virions (WV, also known was intracellular enveloped virus (IEV)), and extracellular virions (EV) [30]. MV contain one membrane layer and normally exit via cell lysis. WV consists of the MV with two additional layers comprised from the Golgi cisternae. The EV is a WV and exits through exocytosis which results in loss of one membrane layer, leaving a MV wrapped in one additional layer [30].

Host antiviral responses

Poxviruses can infect a broad range of vertebrates and invertebrates and hosts must be able to recognize the infection and mount a rapid immune response against it. Poxviruses make viral pathogen-associated molecular patterns (PAMPs) that are sensed by pattern recognition receptors (PRRs): cyclic guanosine monophosphate-adenosine monophosphate (cGAMP) synthase (cGAS), retinoic acid-inducible gene I (RIG-I)- like receptors (RLRs), toll-like receptors (TLRs), and Z-DNA binding protein 1 (ZBP1). One of the ways to sense the viral infection is by sensing of DNA in the cytoplasm. The

cytosolic DNA sensor cGAS binds DNA and synthesizes cGAMP, which then binds to the adaptor protein stimulator of interferon genes (STING), activates the protein kinase IκBα kinase (IKK) and TANK-binding kinase 1 (TBK1), and initiates the activation of IRF3 and NFκB, leading to the induction of cytokines and type I interferons (IFN) [35 – 36] (Fig. 1.1).

The dsRNA produced during intermediate/late gene expression is a potent PAMP, that can be recognized by TLR3 located in endosomes or by RIG-I/melanoma differentiation-associated protein 5 (MDA5) to initiate a fast innate immune response [37 - 38]. RIG-I and MDA5 are classified as RNA helicases that consists of two caspase activating and recruiting domains (CARD) and two helicase domains with an ATP binding domain [39]. RIG-I recognizes short dsRNA containing a 5' triphosphate group on the end and MDA5 recognizes long dsRNA [40 – 42]. Upon activation, RIG-I and MDA5 signal through mitochondrial antiviral signaling (MAVS), and activates TBK1 and IκB kinase-ε (IKKε), which then phosphorylate IRF3/IRF7 and activate NFκB via activation of tumor necrosis factor receptor (TNFR)-associated factor 6 (TRAF6), IKKα, IKKβ and the essential regulatory subunit NEMO [43 – 44], leading to cytokine and IFN production. TLR3 binds dsRNA through the ectodomain (ECD) on TLR3 and recruits Toll/interleukin-1 receptor (TIR) domain containing adapter-inducing interferon-β (TRIF) [38], [45 – 46]. TRIF can then interact with TRAF3, activating TBK1 and IKKε leading to phosphorylation of IRF3 and IFN induction, or TRIF can interact with TRAF6 and activate the IKK complex leading to NFκB activation [47] (Fig. 1.1).

IFNs are cytokines that are produced by cells in response to a variety of stimuli. There are three distinct IFN subtypes, Type I-III. Type I IFNs produce several products

with the best defined being IFN-α and IFN-β (IFNα/β). IFNα/β can then mediate innate and adaptive immune responses, activate the transcription of IFN-stimulated genes (ISGs), and establish an antiviral state in infected and surrounding cells [48]. All nucleated cells have the type I IFN receptor (IFNAR, comprised of IFNAR1 and INFAR2) and can respond to type I IFNs. Once IFNα/β binds to IFNAR it activates the receptor-associated Janus kinase 1 (JAK1) and tyrosine kinase 2 (TYK2) leading to the phosphorylation and dimerization of transcription factor signal transducer and activator of transcription 1 (STAT1) and STAT2, which then assembles with the IFN-regulatory factor 9 (IRF9) and forms the IFN-stimulated gene factor 3 (ISGF3) complex. ISGF3 then binds to the IFN-stimulated response element (ISRE) and activates the transcription of ISGs [48 – 50] (Fig. 1.2).

Type II IFNs are predominantly expressed by T cells and natural killer (NK) cells, producing IFN-γ that can act on a variety of cell types that express the IFN-γ receptor, leading to diverse effects on immune cells to promote adaptive and innate responses [50]. Type III IFNs are produced from a wide range of different cell types and they produce IFN-λ. The IFN-λ receptor is comprised of the specific IFN-λ receptor chain (IFN-λR1 (IL28RA)) and the shared IL-10 receptor chain 2 (IL-10R2 (IL-10Rβ)). Like Type I IFNs, IFN-λs can induce an antiviral state in infected and uninfected neighboring cells, however they primarily target high-risk areas of infection, such as mucosal epithelial cells and they can also act on the human liver. This allows immune protection at mucosal surfaces without the negative inflammatory effects associated with type I IFN responses [51].

The serine/threonine protein kinase R (PKR) and 2', 5' -oligoadenylate synthetase

(OAS) are two IFN-induced enzymes that recognize dsRNA [52 – 54]. PKR binds to dsRNA through its dsRNA binding domains (dsRBDs), dimerizes and autophoshorylates, and goes on to phosphorylate the eukaryotic translation initiation factor 2 (eIF-2α) at residue S51, resulting in the inhibition of protein synthesis, thus inhibiting viral replication [55 – 56]. OAS activation by dsRNA results in the synthesis of 2'-5'-oligoadenylates (2-5As) which activates the cellular endoribonuclease RNase L and leads to the cleavage of viral and cellular RNAs. The cleaved RNA products can then be recognized by PKR, RIG-I, or MDA5 and lead to further antiviral responses [57 – 58].

Another IFN-induced protein is the Z-DNA binding protein 1 (ZBP1, also known as DAI or DLM1). It is a cytosolic innate immune sensor that can recognize dsDNA and Z-form nucleic acids (Z-NAs) and regulate both inflammation and programmed cell death. Z-NAs can be either Z-RNA or Z-DNA that has a left-handed conformational helix, instead of the traditional right-handed helix (B-DNA). Z-NA bases also alternate in an anti- and syn-conformation, resulting in the backbone having a zigzag pattern, hence the name Z-NAs [59 – 61]. B-DNA turns into Z-DNA by flipping the base pairs so they are in an upside down orientation and this causes the phosphate groups to be close together, resulting in an unfavorable high energy conformation [60]. It is now believed that there is a correlation between transcription and Z-DNA formation that is regulated by torsional strain [62 – 64]. ZBP1 contains two Z-DNA/RNA binding domains (Zα1/Zα2) in its N-terminus to bind Z-DNA/RNA and two RIP homotypic interaction motif (RHIM) domains at the center to interact with other RHIM containing proteins [59], [65 – 66]. Once ZBP1 is activated, it can initiate the IRF3 and NFκB pathways that are dependent on the adaptor receptor-interacting protein kinase 1 (RIPK1) binding to the RHIM

domain of ZBP1, leading to the production of type I IFN [66]. Activated ZBP1 can also initiate the necroptosis pathway and lead to cell death.

Necroptosis

For many years, apoptosis was thought to be the sole mechanism of cell death. Apoptosis can stop pathogen infections by killing the cell in a caspase-dependent manner that is non-inflammatory. On the contrary, necroptosis is a caspase-independent process that leads to rupture of the plasma membrane releasing the cellular content in an inflammatory way. Necroptosis can be activated in apoptotic inhibiting conditions through various mechanisms, leading to rapid cell death (Fig. 1.3). The canonical and most studied necroptosis pathway is the tumor necrosis factor alpha (TNF-α) receptor system. It was originally discovered in mouse fibroblasts treated with TNF-α and infected with VACV, which resulted in necroptotic cell death due to the caspase inhibitor in VACV [67]. The TNF-α pathway can lead to cell survival, apoptosis, or necroptosis depending on which complex is formed: complex I (prosurvival), complex IIa (apopototic), or complex IIb (necrosome). Complex I consists of TNFR1, TRADD, RIPK1, TRAF2/5, cIAP1/cIAP2, leading to the ubiquitination of RIPK1 and activation of the NFκB pathway. Complex IIa contains TRADD, RIPK1, FADD, and caspase 8 and if NFκB is activated by complex I, complex II will contain the caspase 8 inhibitor cellular FLICE-like inhibitory protein ($cFLIP_L$) and the cell survives [68]. Caspase 8 induces apoptosis and it also blocks necroptosis by inhibiting RIPK1 and RIPK3. If caspase 8 is inhibited, RIPK1 can be activated through deubiquitination by cylindromatosis (CYLD) and can activate RIPK3 through RHIM-RHIM interaction, leading to RIPK3 autophosphorylation and the formation of complex IIb, known as the necrosome [69],

[70]. The necrosome consists of RIPK1, RIPK3, and FADD and allows phosphorylation of mixed lineage kinase domain-like protein (MLKL) at T357/S358 by RIPK3. MLKL consists of a C-terminal pseudokinase domain and N-terminal four-helix bundle (4HB) domain that undergoes a conformational change upon phosphorylation by RIPK3 exposing the 4HB domain. Positively charged amino acids on the 4HB domain interacts with phosphatidylinositol phosphates (PIPs) and allows MLKL recruitment to the plasma membrane [71], where TAM (Tyro3, Axl, and Mer) kinases phosphorylate T376, allowing for MLKL trimerization and plasma membrane rupture [72 – 75].

Another way necroptosis is activated is through dsRNA binding to TLR3, leading to TRIF interaction with RIPK3 through RHIM-RHIM interaction. RIPK3 autophosphorylates and phosphorylates MLKL, which travels to the plasma membrane and ruptures the cell. TLR4 activates necroptosis through a similar TRIF-RIPK3 pathway, however, it is activated by lipopolysaccharides (LPS) [76 – 77].

ZBP1 has been shown to initiate RIPK3-dependent necroptosis following infection with influenza A virus (IAV), mutant murine cytomegalovirus (MCMV), or mutant VACV [78 – 81]. Lastly, PKR has been implicated in necroptosis by interacting with RIPK1 and RIPK3 when FADD or caspases are inhibited [82].

Innate immune evasion protein, E3

The E3 protein of poxviruses contain a Z-NA binding domain (Z-BD) that shares homology to the Z-BD of adenosine deaminase acting on RNA 1 (ADAR1), ZBP1, and protein kinase containing Z-DNA binding domain (PKZ) [83]. The N-terminus of E3 contains the Z-BD and the C-terminus contains a double stranded RNA binding domain (dsRBD), and it's been shown to be essential for inhibiting the IFN response [84], PKR

inhibition [84 – 88], and for pathogenesis [89]. The VACV N-terminus of E3 has also been shown to be required to inhibit necroptosis and for IFN resistance in L929 cells. VACV mutants that had the entire Z-BD domain deleted, underwent necroptosis that was ZBP1- and RIPK3- dependent [81]. The E3L gene leads to expression of two protein isoforms: one full-length 190-amino acid protein (p25), and a smaller truncated protein missing 37 N-terminal amino acids (p20). The E3 homologue in MPXV, F3, makes only the truncated p20 protein, retaining the fully functioning C-terminal dsRBD and a truncated Z-BD at the N-terminus. Genomic sequencing revealed that E3 and F3 are 92% identical at the nucleotide level and 88% at the protein level [90].

Viral inducer of RIPK3 degradation (vIRD)

Recently, Liu et al. identified a viral inducer of RIPK3 degradation (vIRD) in cowpox virus (CPXV) that inhibits necroptosis and allows for CPXV replication [94]. The N-terminus of vIRD has six ankyrin repeats that are essential for RIPK3 binding and a C-terminal F-box binds to the host SKP1-Cullin1-F-box (SCF) complex and initiates protein ubiquitination and proteasome degradation. vIRD interacts with the C-terminal of RIPK3 containing the RHIM domain and not the N-terminal kinase domain. Through genome analysis, they also identified other orthopoxviruses that contain vIRD orthologs and they include VARV, MPXV, and mouse ectromelia virus (ECTV). VACV lacks an intact vIRD and utilizes other methods for necroptosis inhibition.

In this study we examine the host response to MPXV and VACV E3 N-terminal deletion mutants in L929 and JC cells. We also looked at how MPXV has evolved to remain pathogenic despite having a truncation in the virulence factor, F3.

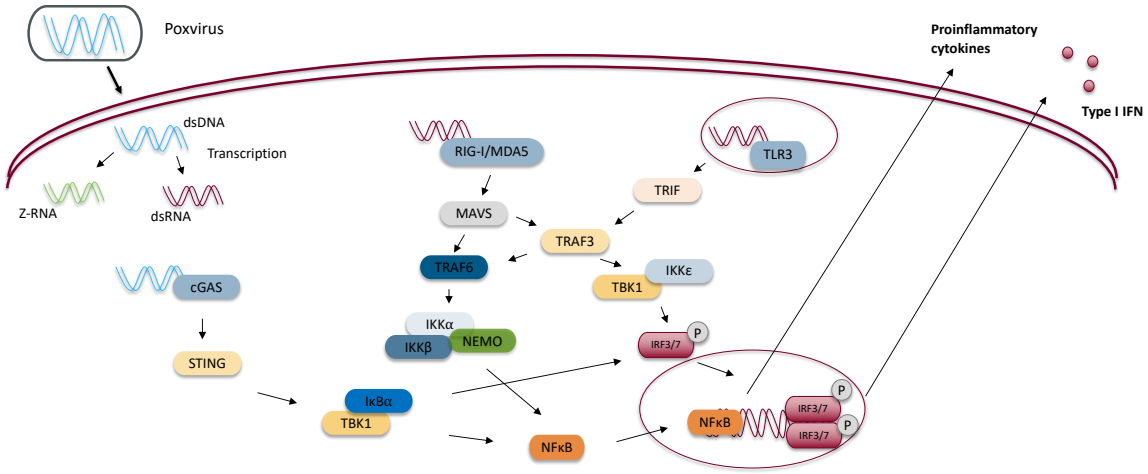

Figure 1.1 Poxvirus sensing pathways. The host can activate antiviral pathways by recognizing dsDNA or dsRNA through cGAS, RIG-I/MDA5, or TLR3. These lead to the activation of NFκB and IRF3/7 leading to the production of proinflammatory cytokines and Type I IFNs that act on surrounding cells.

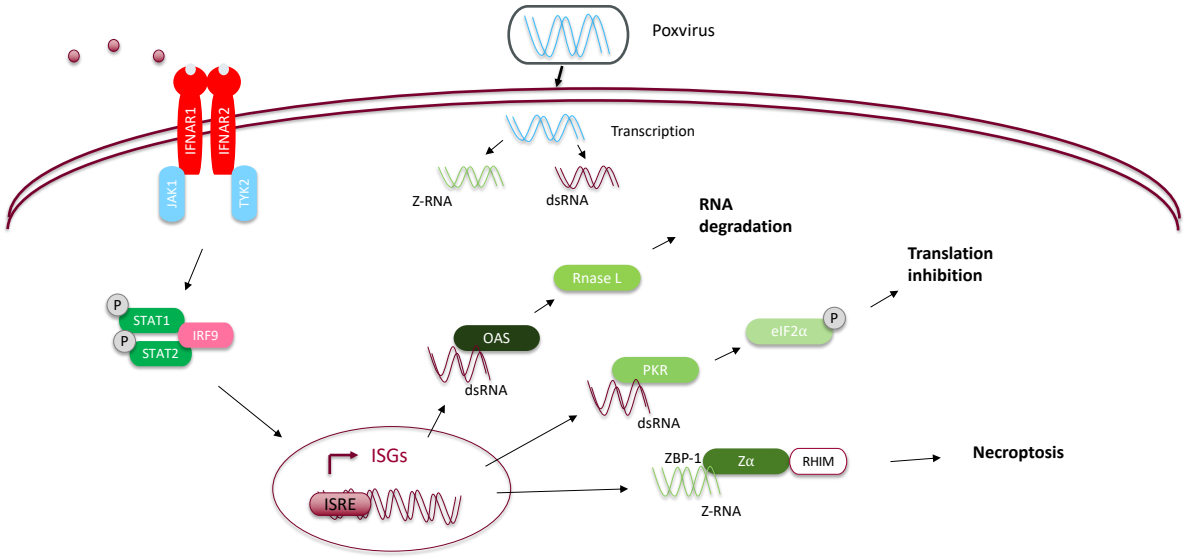

Figure 1.2 Type I IFN response. Type I IFNs bind the IFN receptor (IFNAR1/IFNAR2) and signal through the JAK/STAT pathway to activate ISGs, leading to the upregulation of OAS, PKR, and ZBP1, which leads to the activation of different antiviral pathways.

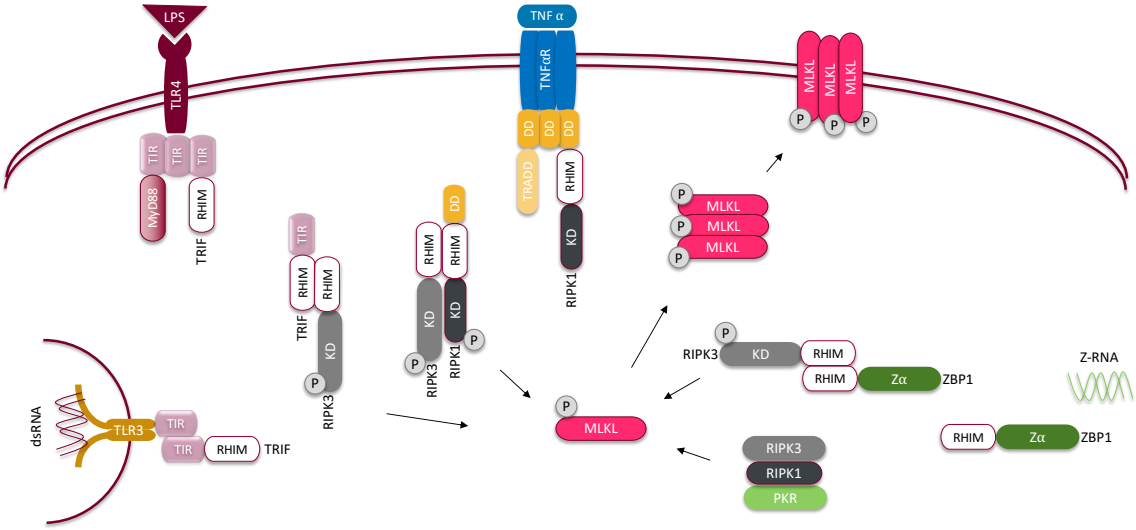

Figure 1.3 Activating necroptosis. Necroptosis can be activated by TLR3, TLR4, TNFα/TNFαR, ZBP1, or PKR. All of these activate RIPK3 through RHIM-RHIM interaction, which phosphorylates MLKL, leading to MLKL aggregation and cell death through loss of membrane integrity.

CHAPTER 2

REGULATION OF NECROPTOSIS AND THE TYPE I INTERFERON RESPONSE BY MONKEYPOX VIRUS

ABSTRACT

Monkeypox (MPXV) has re-emerged as the most important orthopoxvirus infection of humans. Despite being highly pathogenic, it contains a natural truncation at the N-terminus of its E3 homologue leading to the loss of the first 37 amino acids. Our previous data have shown that vaccinia virus (VACV) E3 protein is required for interferon-resistance of VACV. The N-terminal Z-nucleic acid binding domain is necessary to inhibit induction of necroptosis, as VACV containing an N-terminal deletion (VACV-E3LΔ37N) undergoes rapid ZBP1-dependent necroptotic cell death, through activation of RIPK3, and subsequent phosphorylation and trimerization of the executioner of necroptosis, MLKL. Despite lacking parts of the N-terminus, MPXV has evolved ways in circumventing necroptotic cell death in mouse L929 cells. Our data shows that MPXV infection leads to delayed phosphorylation of MLKL but does not lead to MLKL trimerization, nor cell death. We show that MPXV inhibits necroptosis in two steps: by degrading RIPK3 through either a caspase-dependent pathway or through the "viral inducer of RIPK3 degradation" (vIRD) and by inhibiting MLKL aggregation. Additionally, MPXV shows interferon sensitivity that is fully ZBP1- and RIPK3- and MLKL-dependent, but independent of necroptosis. Addition of a pancaspase inhibitor (zVAD) or a proteasome inhibitor (MLN4924) does not increase cell death but leads to an increase in interferon sensitivity comparable to VACV-E3LΔ37N. Thus, treatment

with an interferon inducer along with a pancaspase or proteasome inhibitor could potentially be a beneficial treatment against MPXV infections.

INTRODUCTION

Monkeypox virus (MPXV) is an orthopoxvirus that causes smallpox-like disease which has up to a 10% mortality rate, depending on the infectious strain [1]. The global eradication of the smallpox virus has led to the decrease in smallpox vaccinations, which over the years has led to a drastic increase in the number of human MPXV cases [2]. Recently, the Global Commission for the Certification of Smallpox Eradication has named MPXV as the most important orthopoxvirus to infect humans since the eradication of smallpox. In the past MPXV has remained mainly endemic to Western and Central Africa with recent sporadic cases linking back to travelers who had visited Nigeria. The first MPXV outbreak in the U.S. occurred in 2003 and was traced back to an infected rodent imported from Africa [3]. There were also other isolated cases of MPXV spread from 2018-2021 to Israel, the UK, Singapore, and U.S. [4 – 7]. In 2022, we have seen the first MPXV case in a person who has not traveled to Africa, and as of July 2022, there have been 6,027 confirmed cases in 59 countries [8].

The high rate of transmission of MPXV around the world has become alarming. There are currently two vaccines available that are effective against MPXV: JYNNEOS™ (live, replication incompetent vaccinia virus (VACV)) and ACAM2000® (live, replication competent VACV) [9], however they may be available in limited supplies. According to the Centers for Disease Control and Prevention (CDC), there is no specific treatments specifically against MPXV infections, but there are antiviral drugs that have been shown to be effective against orthopoxviruses. The antiviral ST-246 (also known as Tecovirimat or TPOXX) has been the current drug of choice [9 – 10], and brincidofovir and cidofovir are also approved but data showing effectiveness against

MPXV infections is lacking [9]. Given the limited number of antivirals specific against MPXV, development of additional anti-orthopoxvirus drugs would be highly beneficial in combating the current MPXV outbreak. In this chapter, we show that an interferon inducer, either with a pancaspase inhibitor or a proteasome inhibitor, could potentially be used as a potential treatment against MPXV infection.

Much of our knowledge of orthopoxvirus pathogenesis and immune evasion comes from the study of VACV. The E3 protein of VACV has been shown to be essential for inhibiting the cell's antiviral interferon (IFN) response [11], for PKR inhibition [11 – 15], and for pathogenesis [16]. The E3 protein is comprised of two conserved domains: the N-terminal Z-form nucleic acid (Z-NA) binding domain (known as ZBD or Zα) and the C-terminal double-stranded RNA (dsRNA)-binding domain (dsRBD). Expression of the E3L gene leads to formation of two protein isoforms, one full-length 190-amino acid protein that contains both N- and C- terminal domains (p25), and a smaller protein that is truncated of 37 N-terminal amino acids (p20), which is the result of leaky scanning past the first AUG start codon (p20). A genomic sequence comparison between MPXV and VACV showed that the E3 homologue of MPXV, F3, is 92% similar at the nucleotide level and 88% at the protein level to the VACV E3 protein. The F3 protein retains a complete, fully functional dsRBD, however, the first 37 amino acids of the N-terminal ZBD are missing, resembling the smaller p20 VACV E3 protein [17].

Apoptosis and necroptosis are linked pathways that result in cell death. In apoptotic conditions, active caspase-8 will cleave and inactivate receptor interacting protein kinase 1 (RIPK1) and RIPK3 leading to apoptosis [18]. When caspase 8 is

inhibited, RIPK1 and RIPK3 form a complex leading to the phosphorylation and oligomerization of mixed lineage kinase like-domain protein (MLKL), the final executioner of MLKL [19 – 22]. Phosphorylated MLKL will translocate to the plasma membrane where it trimerizes and permeabilizes the membrane, resulting in cell death [23 – 24]. RIPK1 and RIPK3 each contain a receptor-interacting protein homotypic interaction motif (RHIM) domain that can mediate protein-protein interaction. In addition, a RHIM is present in the TLR-adaptor protein TRIF, as well as Z-DNA binding protein 1 (ZBP1, also known as DAI or DLM1) [25].

We previously showed that the VACV N-terminus of E3 protein is necessary to inhibit IFN-primed necroptosis and for IFN resistance in L929 cells. When L929 cells were pretreated with IFNα and infected with VACV, mutants that were missing part or the entire Z-NA binding domain of E3 (VACV-E3LΔ37N or VACV-E3LΔ83N), showed an IFN sensitive phenotype, compared to wtVACV that was fully IFN resistant. Infection with these VACV mutants also underwent a rapid cell death, necroptosis, that was ZBP1- and RIPK3- dependent [26]. Here, we explore how MPXV responds to the host antiviral IFN pathway and ways it has evolved to remain pathogenic despite having a truncation in its E3 homologue.

MATERIALS AND METHODS

Cell lines and Treatments. Murine fibroblasts L929 were obtained from ATCC and maintained in Eagle's Minimum Essential Medium (MEM) (Corning) supplemented with 5% fetal bovine serum (FBS, HyClone). Cells were maintained in 37℃ in a 5% CO_2 atmosphere. BSC40 cells were maintained in Dulbecco's Modified-Minimal Essential Medium (DMEM), supplemented with 5% FBS. Pretreatment with mouse IFNα (Calbiochem) was used at 100 U/mL for 1 hour prior to viral infections. To inhibit caspase activity, the pancaspase inhibitor, zVAD-FMK (ApexBio) was used at 50 μM for 1 hour prior to and during infection. For TNF-induced necroptosis, zVAD-FMK was used for pretreatment and TNF-α (Sigma) was added at 20 ng/mL. For RIPK3 degradation inhibition, the neddylation inhibitor MLN 4924 (ApexBio) was added at 1 μM for 1 hour prior to and during infection.

Viruses. For wtVACV infections, Western Reserve (WR) strain was used. The VACV mutant containing the 37-amino acid N-terminal deletion of E3 (VACV-E3Δ37N), was constructed as previously described [13], [28]. The MPXV strain used through this paper was WR 7-61 and experiments were performed in accordance with the protocols approved by Arizona State University and the CDC. The CPXV strain used was Brighton red and a kind gift from Grant McFadden's lab. For all infections, an MOI of 5 was used unless otherwise specified.

IFN sensitivity plaque assays. L929 and L929 CRISPR/KO cells were seeded in a 12-well tissue culture plate (VWR) to be 95% confluent on the day of infection and treated with increasing doses of IFNα (0-100U/mL) for 18 hours prior to infection. The cells were then infected with 70 PFU of wtVACV, VACV-E3Δ37N, MPXV, or VACV-

E3Δ26C and infected for 1 hour with rocking every 10 minutes. After 3-4 days, VACV and VACV mutant infections were stained with crystal violet and plaques counted. For MPXV, plaque formation took 6-7 days, then cells were stained with crystal violet and plaques counted.

Cell viability assays. L929 cells were plated on a 48-well CytoOne tissue culture-treated plates (USA Scientific) and pretreated with 100 U of IFNα for 18 hours. Cells were infected with the indicated viruses at an MOI of 5 and incubated at 37℃ for 1 hour with rocking every 10 minutes. After infection, cells were overlayed with MEM that contained Hoechst for nuclear staining, and 1 μM SYTOX Green for membrane integrity. The cells were incubated at 37℃ with 5% CO_2 on an EVOS FL auto imaging microscope (Invitrogen) with an onstage incubator and images were taken every hour for 16 hours.

Growth kinetics. L929 and CRISPR/Cas9 KO cells were seeded on a 12-well tissue culture plate (VWR) to be 80% on the day of infection. After attachment, cells were pretreated with 100 U of IFNα for 18 hours. Cells were infected with the indicated viruses at an MOI of 5 and incubated at 37℃ with 5% CO_2 for 1 hour with rocking every 10 minutes. After infection, the cells were washed 3 times with prewarmed media prior to overlay with growth media. The viral samples were harvested at 1, 24, and 48 hours post infection and underwent 3 freeze/thaws. The viral titers were determined by plaquing in BSC40s followed by crystal violet staining.

Immunofluorescence assay. The LIVE/DEAD Fixable stain kit (ThermoFisher) was used for immunofluorescent (IF) viability assay. L929 cells were seeded to be 90% confluent on the day of infection and pretreated with 100 U of IFNα for 18 hours. Cells

were infected with VACV-E3Δ37N or MPXV at an MOI of 5 and infected for 1 hour, followed by growth media overlay. After 16 hours post infection, cells were washed 3X with prewarmed 1X PBS and LIVE/DEAD green fluorescent dye (1:800) was added and incubated at RT for 30 minutes, protected from light. Cells were washed once with 1X PBS and fixed with 4% formaldehyde and incubated at RT for 15 minutes. Once the formaldehyde was removed, 0.125M Glycine was added to the cells to quench any remaining formaldehyde. The cells were washed 3X with 1X PBS and permeabilized by washing 2X with ice-cold PBS. Blocking was done with 3% BSA, 0.3% gelatin, and 0.1% TritonX-100 (TX-100) at RT for 1 hour. The primary antibody (E3 at 1:250) was added in GT-PBS1 (0.3% gelatin, 0.1% TX-100 in PBS) and incubated overnight at 4℃. The cells were washed 2X with GT-PBS1 and the secondary antibody was added (Texas red at 1:250) in GT-PBS1 at RT in the dark for 2 hours. The cells were washed 1X with GT-PBS1 and 1X with PBS and visualized in the EVOS FL auto imaging microscope.

Protein extraction and Western blot analysis. Cells were seeded in a 12-well tissue culture-treated dish to be 80% confluent on the day of infection. Following viral infection, the cells were scraped, pelleted, washed once with 1X PBS, and lysed in RIPA lysis buffer (150 mM NaCl, 1% P-40, 0.5% sodium deoxycholate, 0.1% SDS, 25 mM Tris pH 7.4) with 1X Halt Protease and Phosphatase Inhibitor Cocktail (Thermo Scientific) and incubated on ice for 5 minutes. For phosphorylated MLKL, QIAshredder columns (Qiagen) were used following cell lysis. Proteins were separated on SDS/Page, transferred to a nitrocellulose membrane with 10 mM 3-(cyclohexylamino)-1-propane sulfonic acid (CAPS), 20% methanol, pH 11 at 100V for 1 hour and 15 minutes, and blocked in 3% bovine serum albumin (BSA). For trimerized MLKL samples, SDS/Page

was run under non-reducing conditions and the proteins were transferred at 70V for 3 hours. The following antibodies were used: ZBP1 (Zippy-1, Adipogen), RIPK3 (ProSci), pMLKL (abcam), MLKL (Cell Signaling Technology), β-Actin (Santa Cruz Biotechnology), and PKR (Santa Cruz Biotechnology). Secondary antibodies were goat anti-rabbit IgG or goat anti-mouse IgG (Cell Signaling Technology), depending on the primary antibody used. The proteins were visualized by chemiluminescence with either SuperSignal West Pico PLUS or Dura substrate (ThermoFisher).

MLKL localization with TX-114. Cells were seeded on 6-well tissue culture-treated plates to be 80% confluent on the day of infection and pretreated with 100 U IFNα. After infection, the cells were scraped, pelleted, and washed with cold 1X PBS, and lysis buffer was added (20mM HEPES, 150 mM NaCl, 2% Triton X-114) and incubated on ice for 30 minutes. The samples were then centrifuged at 15,000 x g for 5 minutes at 4℃, the supernatant was harvested and incubated at 37℃ for 5 minutes, followed by centrifugation at 1,500 x g for 5 minutes at room temperature. The top aqueous layer was separated, additional TX-114 lysis buffer was added and the samples were incubated at 37℃ for additional 3 minutes, followed by centrifugation at 1,500 x g for 5 minutes to remove any contamination from the detergent layer. The samples were saved as Aq samples. The detergent enriched layer was diluted with basal buffer (20 mM HEPES, 150 mM NaCl) to the same volume as the detergent soluble fraction, incubated at 4℃ for 15 minutes, incubated at 37℃ for 3 minutes and centrifuged at 1,500 x g for 5 minutes. The samples were diluted with basal buffer to the same volume as the Aq samples and saved as Det. The proteins were then visualized by Western blot as described above.

L929 CRISPR KO cell lines. L929 cells were transduced with Edit-R Lentiviral particles containing Cas9 sgRNA (Horizon Discovery) according to manufacturer's instruction and expression of Cas9 was verified by Western blot. The Cas9 expressing L929 cells were then transduced to KO the following proteins: ZBP1, RIPK3, PKR, and MLKL. The cells were infected with Edit-R Lentiviral specific sgRNAs (Horizon Discovery) at an MOI of 0.3 and the remaining protocol was followed according to the manufacturer's instruction. The protein KOs were confirmed via Western blot.

RESULTS

MPXV is IFN sensitive and does not induce cell death. Since the E3 homologue in MPXV has a natural truncation at the N-terminus similar to VACV-E3LΔ37N, we wanted to see if MPXV was IFN-sensitive in L929 cells, similar to what our lab had previously observed with VACV N-terminal mutants, VACV- E3LΔ37N and VACV-E3LΔ83N [26], which are missing all or part of the N-terminal Z-NA binding domain of E3. L929 cells were pretreated with increasing doses of mouse IFNα for 18 hours and infected with 100 plaque forming units (PFU) of wtVACV, VACV-E3LΔ37N, or MPXV. As shown in Fig. 2.1A, wtVACV is fully IFN resistant, VACV-E3LΔ37N is IFN sensitive, and MPXV is IFN sensitive with an intermediate phenotype between wtVACV and VACV-E3LΔ37N. These data show that in L929 cells, IFNα can reduce plaque formation of MPXV with 10 U of IFN reducing plaques by about 50%.

IFN-sensitivity of VACV- E3LΔ37N and VACV- E3LΔ83N is associated with ZBP1-dependent necroptotic cell death [26 – 27]. The ability of MPXV to induce cell death was examined using live imaging in IFN-primed L929 cells. The cells were pretreated with 100 U of mouse IFNα for 18 hours and infected with VACV-E3LΔ37N or MPXV at an MOI of 5 and the cells were visualized every hour. Cell viability was examined by examining plasma membrane integrity using a SYTOX exclusion assay. Despite having a natural truncation in the N-terminus of the E3 homologue, MPXV infection does not lead to rapid cell death, like we see with VACV-E3LΔ37N (Fig. 2.1B). At 16 hours post infection, the majority of the L929 cells infected with MPXV stained positive for E3 (red staining) while very few cells stained green for dead cells, compared to VACV-E3LΔ37N (Fig. 2.1C and D, respectively). This data demonstrated that the

lack of cell death is not due to absence of virus infection. This also indicates that MPXV has evolved mechanisms of immune evasion independent of the E3 homologue.

We have also evaluated MPXV replication in L929 cells under single cycle replication conditions, in the presence and absence of IFN. A viral growth curve was performed in which the cells were pre-treated with 100 units of IFN for 18 hours and infected with VACV-E3LΔ37N, wtVACV, or MPXV at an MOI of 5 and the samples were harvested at 1, 24, and 48 hours post infection. The viral titers were then determined by plaquing in BSC40 cells. In the absence of IFN, VACV-E3LΔ37N and MPXV grew by 1-log and wtVACV grew 1.5-logs (Fig. 2.1E). In the presence of IFN, both VACV-E3LΔ37N and MPXV failed to replicate while wtVACV titers increased 2-logs (Fig. 2.1F). This data shows that IFNα can efficiently inhibit MPXV viral replication *in vitro* under single cycle conditions.

IFN sensitivity is dependent on ZBP1, RIPK3, and MLKL but not PKR. IFN-sensitivity of E3LΔ37N and VACV-E3LΔ83N is dependent on the ZBP1/RIPK3/MLKL pathway. We wanted to ask if IFN sensitivity of MPXV was dependent on ZBP1, RIPK3, and MLKL, despite not leading to necroptotic cell death. CRISPR/Cas9 L929 cells that failed to make these proteins (Fig. 2.2A) were seeded and pretreated with increasing doses of IFNα (0-100 U/mL) for 18 hours. IFN sensitivity was examined by infecting CRISPR KO L929 cells with 100 PFU of wtVACV, VACV-E3LΔ37N, VACV-E3LΔ26C, or MPXV. All viruses were IFN resistant upon deletion of ZBP1, and replicated efficiently in the presence of IFN, except for VACV-E3LΔ26C (Fig. 2.2B). VACV-E3LΔ26C has 26 amino acids deleted from the C-terminus of E3, which is the dsRNA-binding domain and is required for inhibition of IFN-inducible

dsRNA-sensing pathways, PKR and OAS and IFN resistance, but not for inhibition of necroptosis [12], [26], [28]. Similar results were seen in RIPK3 knock-out L929 cells (Fig. 2.2C). In the L929 MLKL KOs, the IFN sensitivity of MPXV is completely dependent on MLKL. MPXV IFN resistance increased to wtVACV levels but the N-terminal mutants, VACV-E3LΔ37N and VACV-E3LΔ83N, increased to 100% resistance with 1 U of IFN and decreased slightly to give 50% resistance at 100 U of IFN. This could be due to ZBP1 and RIPK3 acting in another pathway beyond necroptosis, such as NFkB, apoptosis, or inflammation. VACV-E3LΔ26C remained IFN sensitive, as expected (Fig. 2.2D). We tested PKR knock-out cells as a control since induction of necroptosis in L929 cells by E3LΔ37N and VACV-E3LΔ83N has been shown to be PKR-independent [27]. When PKR was knocked out of L929 cells, the presence of IFN in the cells was able to limit viral replication of VACV- E3LΔ37N and to an intermediate level MPXV, similar to WT L929 cells, despite PKR being absent (Fig. 2.2E). This demonstrates PKR is dispensable for IFN sensitivity of MPXV in L929 cells.

We confirmed that ZBP1, RIPK3, and MLKL is required for IFN resistance by looking at viral growth in a 1-step growth curve. The KO cells were pretreated with IFN infected with VACV- E3LΔ37N, wtVACV, or MPXV at an MOI of 5. The cells were harvested at the indicated time points and the viruses were plaqued in BSC40s to determine the viral titers. VACV- E3LΔ37N replicated 1.5-logs in ZBP1 KO, 2-logs in RIPK3 KO, and 3-logs in MLKL KO cells. wtVACV replicated 2-logs in all the KO cells, and MPXV replicated 1.5-logs in ZBP1 and MLKL KO cells and 2-logs in RIPK3 KO cells (Fig. 2.2F-G). Thus, MPXV and VACV- E3LΔ37N viral replication in the presence of IFN is dependent ZBP1, RIPK3, and MLKL.

MPXV vIRD leads to RIPK3 cleavage and inhibition of necroptosis. We have previously showed that the E3 protein of VACV is necessary to inhibit viral-induced ZBP1-dependent necroptosis, as the E3 N-terminus deletion mutants caused rapid cell death due to phosphorylation and trimerization of MLKL in L929 cells [26]. We were interested in seeing if MLKL becomes phosphorylated and trimerizes in cells infected with MPXV, since MPXV contains a truncated N-terminal E3 homologue, similarly to the VACV-E3LΔ37N construct. We infected L929 cells with MPXV and VACV-E3LΔ37N and harvested the viral samples at 2, 4, and 6 hours post infection and the samples were run on a Western blot with antibodies against phosphorylated MLKL. We were able to detect phosphorylated MLKL as early as 2 hours post infection with VACV-E3LΔ37N, but in MPXV infected cells, it was not detected until 6 hours post infection (Fig. 2.3A). Since the last step in necroptosis after phosphorylation of MLKL is trimerization of MLK, we looked at the trimerization status in MPXV infected cells. Trimerization of MLKL was detected with VACV-E3LΔ37N but not with MPXV at 10 hours post infection (Fig. 2.3B). These data indicate that phosphorylation of MLKL is not sufficient to induce necroptosis in MPXV infected cells and MPXV inhibits necroptosis downstream of MLKL phosphorylation as we do not detect MLKL trimerization.

Since necroptosis is a highly inflammatory process, cells need a way to inhibit this pathway during unnecessary times. Caspase-8 has been shown to inhibit necroptosis by cleaving RIPK3 and deletion of caspase-8 is lethal in mice embryos which can be rescued by deletion of RIPK3 or MLKL [18], [29 – 32]. Inhibition of necroptosis has also been shown to occur with cowpox virus (CPXV) infections through its “viral inducer

of RIPK3 degradation" (vIRD). The vIRD contains six ankyrin repeats at the N-terminus and an F-box at the C-terminus. It was shown to bind the host SKP1-Cullin1-F-box (SCF) machinery to target RIPK3 for proteasomal degradation [33]. We wanted to ask if the reason MPXV was not inducing necroptosis was because RIPK3 is being degraded. As shown in figure 2.3C, RIPK3 was expressed in mock treated, wtVACV, and VACV-E3LΔ37N to high levels, as expected, because VACV vIRD is truncated and missing the C-terminal F-Box [33]. In MPXV treated cells, RIPK3 levels were significantly decreased compared to mock treated and VACV infected cells and in the CPXV samples, RIPK3 was completely degraded. We pretreated L929 cells with zVAD-FMK to see if inhibition of caspases would restore RIPK3 levels. In mock treated, TNF/zVAD, wtVACV, and VACV-E3LΔ37N infected cells RIPK3 levels were present in high amounts and addition of zVAD restored RIPK3 levels in MPXV and CPXV infected cells (Fig. 2.3D). Addition of zVAD also increased the time of detection of phosphorylated MLKL in MPXV infected cells from 6 hours to 4 hours (Fig. 2.3A), but did not lead to trimerization of MLKL (Fig. 2.3B) or necroptotic cell death. This shows that MPXV reduces RIPK3 levels to inhibit necroptosis MLKL phosphorylation.

Next, we used the neddylation inhibitor, MLN4924 (ApexBio), to inhibit RIPK3 degradation and induce necroptosis in MPXV and CPXV infected cells [33]. L929 cells were pretreated with MLN4924 and infected with the indicated viruses (MOI 5) for 16 hours and RIPK3 levels were analyzed via western blot. Mock, wtVACV, and VACV-E3LΔ37N expressed RIPK3 to high levels and addition of MLN4924 restored RIPK3 levels in MPXV and CPXV infected cells (Fig. 2.3E). Necroptosis was investigated by infecting with the indicated viruses (MOI 5) with or without MLN4924 and cell death

was measured at 16 hours post infection. Mock and MLN4924 treated cells showed no toxicity, TNF/zVAD treated cells underwent necroptosis, wtVACV and wtVACV with the addition of MLN4924 did not induce cell death, while VACV-E3LΔ37N induced necroptosis that was not affected by MLN4924. In MPXV infected cells, cell death was not detected with or without MLN4924, but in CPXV infected cells, only with the addition of MLN4924 did we observe a decrease in cell viability (Fig. 2.3F). We confirmed necroptosis by performing a western blot and probing for phosphorylated and trimerized MLKL. Cells infected with CPXV showed phosphorylated and trimerized MLKL only with the addition of MLN4924. Cells infected with wtVACV had no phosphorylated or trimerized MLKL and addition of MLN4924 to VACV-E3LΔ37N infected cells gave a stronger signal for phosphorylated and trimerized MLKL. Addition of MLN4924 to MPXV infected cells gave phosphorylated MLKL but not trimerized MLKL (Fig. 2.3G). This data suggests that the MPXV vIRD cleaves RIPK3 and inhibits MLKL phosphorylation.

Caspase and neddylation inhibition leads to increased IFN sensitivity of MPXV but does not lead to necroptosis. The default death pathway for virally infected cells is apoptosis. When caspase-8 is inhibited, RIPK3 can be activated through RHIM interactions with RIPK1, ZBP1, or TLR3/TLR4 (TRIF) and lead to MLKL activation and cell death. We wanted to see if we could induce necroptosis in MPXV infected cells with the addition of the pancaspase inhibitor, zVAD-FMK. The addition of zVAD to our cell viability assay had no significant effect on cell survival in MPXV or VACV-E3Δ37N infected cells, as measured by SYTOX green uptake. Despite inhibiting RIPK3 cleavage in MPXV infected cells, there was no increase in cell death (Fig. 2.4A). Next, we looked

at the IFN sensitivity of MPXV with the pancaspase inhibitor. The intermediate IFN sensitivity of MPXV was increased with the addition of zVAD to IFN treated L929 cells. Without zVAD, approximately 50% plaque reduction was observed with 10 U of IFN in the case of MPXV, whereas VACV-E3LΔ37N required only 3 U of IFN. Treatment with zVAD increased IFN sensitivity of MPXV infected cells to resemble VACV-E3LΔ37N with 3 U of IFN giving a 45% plaque reduction. Treatment of zVAD had no effect on IFN sensitivity with VACV-E3LΔ37N (Fig. 2.4B). Addition of MLN4924 also increased IFN sensitivity of MPXV and VACV-E3LΔ37N infected cells, with 1 U of IFN reducing plaque formation by 50% (Fig. 2.4C). These results demonstrated that the addition of the pancaspase inhibitor, zVAD, or the neddylation inhibitor, MLN4924, can effectively enhance the IFN sensitivity of MPXV.

Caspase and neddylation inhibition leads to MLKL membrane localization without necroptosis. Since in MPXV- infected cells, we were unable to visualize MLKL aggregation, we wanted to visualize where the MLKL inhibition step was occurring. We infected L929 cells with the indicated viruses and used Triton X-114 (TX114) in our lysis buffer. TX114 is a non-ionic detergent which separates the samples into aqueous (Aq) and detergent (Det) phases when the samples are heated above 22℃. The Aq samples will then contain the hydrophilic solutes while the Det samples will contain the hydrophobic solutes [34], allowing us to follow phosphorylated MLKL from the cytoplasm to the membrane in MPXV infected cells. In TNF/zVAD treated samples, phosphorylated MLKL is detected in the Aq samples with a stronger signal in the Det samples. In wtVACV samples, no phosphorylation of MLKL is detected, consistent with our data that it does induce necroptosis. In VACV N-terminal deletion mutants,

phosphorylated MLKL is detected in the Aq and Det samples, but the signal is stronger with the addition of zVAD. In MPXV infected cells, phosphorylated MLKL is not detected in the Aq or Det phase, but it is clearly visible with the addition of zVAD starting at 6 hours post infection (Fig. 2.4D). Addition of MLN4924 gave similar results showing phosphorylated MLKL localizing to the membrane in MPXV and VACV-E3LΔ37N infected cells (Fig. 2.4E). Therefore, phosphorylated MLKL is slightly delayed in MPXV infected cells and is localized from the cytoplasm to the membrane, but only in the presence of the pancaspase inhibitor zVAD or the neddylation inhibitor.

DISCUSSION

Many viruses activate the host type I IFN pathway, leading to the upregulation of interferon stimulated genes (ISGs). These ISGs encode different antiviral pathways that regulate different aspects of the viral lifecycle, such as PKR, OAS, and ZBP1. Viruses, on the other hand, have evolved ways to circumvent these pathways. The VACV E3 protein has been shown to bind dsRNA and sequester it away from PKR and OAS [11]. E3 also sequesters Z-RNA to prevent activation of ZBP1 [27] and is necessary for IFN resistance [11]. The E3 homologue in MPXV is naturally truncated at the N-terminus, but it is still able to inhibit antiviral immune responses to at least some extent [17]. In this manuscript, we show that the addition of IFNα effectively inhibits MPXV viral replication *in vitro* in L929 cells. MPXV is also IFN sensitive in a plaque reduction assay in that increasing IFN doses prevents viral spread to surrounding cells. Addition of 10 U of IFNα is able to decrease the plaque formation by 50%. Thus, MPXV is the first orthopoxvirus characterized to be IFN-sensitive in cells in culture. IFN sensitivity of MPXV is dependent on ZBP1, RIPK3, and MLKL, but not on PKR as knocking out ZBP1, RIPK3, or MLKL fully restored IFN resistance of MPXV, but MPXV remained IFN sensitive in the PKR KOs. It was surprising that the IFN sensitivity was dependent on ZPB1, RIPK3, and MLKL, since MPXV did not induce necroptosis. West Nile virus has been shown to be restricted in neurons in a RIPK3-dependent manner that is independent of cell death and results in chemokine production [35]. Zika virus infection in neurons also leads to ZBP1- and RIPK-dependent inhibition in the absence of necroptosis. ZBP1 and RIPK1/RIPK3 activated a restrictive antiviral state by inducing IRG1 to produce itaconate, which inhibited viral replication [36]. Further MPXV

experiments aim to study how the IFN sensitivity is dependent on necroptosis proteins in the absence of cell death.

In addition to not inducing necroptosis, MPXV infection led to delayed MLKL-serine phosphorylation. The delay in MLKL phosphorylation was due to degradation of RIPK3 in MPXV-infected cells. Phosphorylation of MLKL could be at least partially restored either by treating with a pancaspase inhibitor, zVAD to inhibit caspase dependent degradation of RIPK3 or treating with a proteosome inhibitor, MLN4924, to inhibit the vIRD dependent degradation of RIPK3. Despite restoring MLKL-phosphorylation, neither treatment with zVAD nor MLN4924 induced cell death in MPXV infected cells. Treatment with zVAD led to MLKL-phosphorylation, migration of phosphorylated MLKL to membranes, but not trimerization nor cell death. Similarly, treatment with MLN4924 led to increased MLKL phosphorylation but no trimerization. This suggests that MPXV has evolved mechanisms to inhibit necroptosis downstream of MLKL phosphorylation.

While zVAD treatment did not increase induction of necroptotic cell death it did increase sensitivity of MPXV to IFN-treatment. At a concentration of 10 U of IFNα, zVAD addition increased MPXV sensitivity from 50% plaques to 10%. This data shows the potential that a pancaspase inhibitor in conjunction with IFN-treatment, or treatment with an IFN-inducer could be used as a MPXV treatment in infected individuals. Future MPXV experiments are planned to test an IFN enhancer with and without a pancaspase inhibitor in an *in vivo* model.

MPXV contains a functional vIRD protein that leads to RIPK3 cleavage and inhibition of necroptosis. We show that RIPK3 expression in MPXV infected cells is

greatly reduced compared to VACV and mock infected cells, however it is not completely degraded as in CPXV infected cells. This could be due to a timing issue and at later times post infection, we expect RIPK3 to be completely degraded in MPXV-infected cells. Inhibition of the host SKP1-Cullin1-F-Box (SCF) machinery by the neddylation inhibitor, MLN4924, did not lead to necroptosis as shown by cell viability assay. We observed the same phenomenon as we saw with the addition of the pancaspase inhibitor, zVAD-FMK, in that MLKL gets phosphorylated and travels to the membrane but does not trimerize or cause cell death. MLKL trimerization is the last step in necroptosis required for cell lysis [23 – 24]. Thus, even if the host is able to inhibit RIPK3 degradation, MPXV has evolved an additional way to inhibit necroptosis through an unknown mechanism inhibiting MLKL trimerization and cell lysis. Further studies aim to identify the late inhibition of necroptosis downstream of MLKL phosphorylation and characterize the interferon sensitivity in the absence of death.

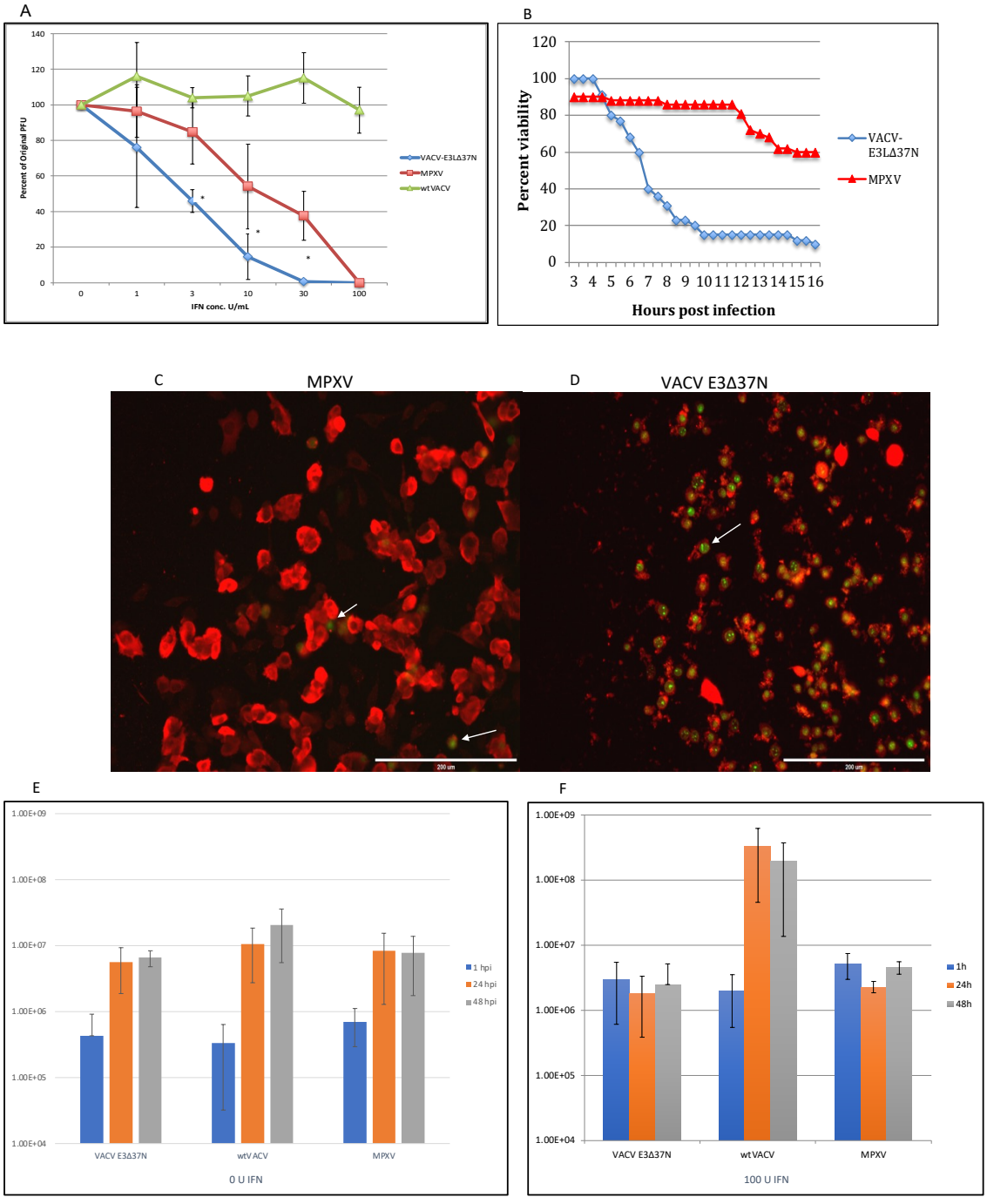

Figure 2.1. MPXV is IFN sensitive and does not induce cell death. A) IFN plaque reduction assay showing MPXV has an intermediate IFN phenotype between wtVACV and VACV-E3Δ37N. B) SYTOX green cell viability assay showing VACV-E3Δ37N undergoes rapid cell death and MPXV does not. C-D) IF with LIVE/DEAD green

fixable stain to visualize infected and dead cells infected with MPXV and VACV-E3Δ37N. The red is stained for E3 and the green is dead cells. The white arrow show dead cells. E) 1-step viral growth curves with wtVACV, VACV-E3Δ37N, and MPXV at an MOI of 5 and harvested at 1, 24, and 48 hours post infection and plaqued in BSC40s. F) Same as E, except cells were pretreated with 100 U of IFNα for 18 hours. *p=<.05 when comparing VACV-E3Δ37N and MPXV.

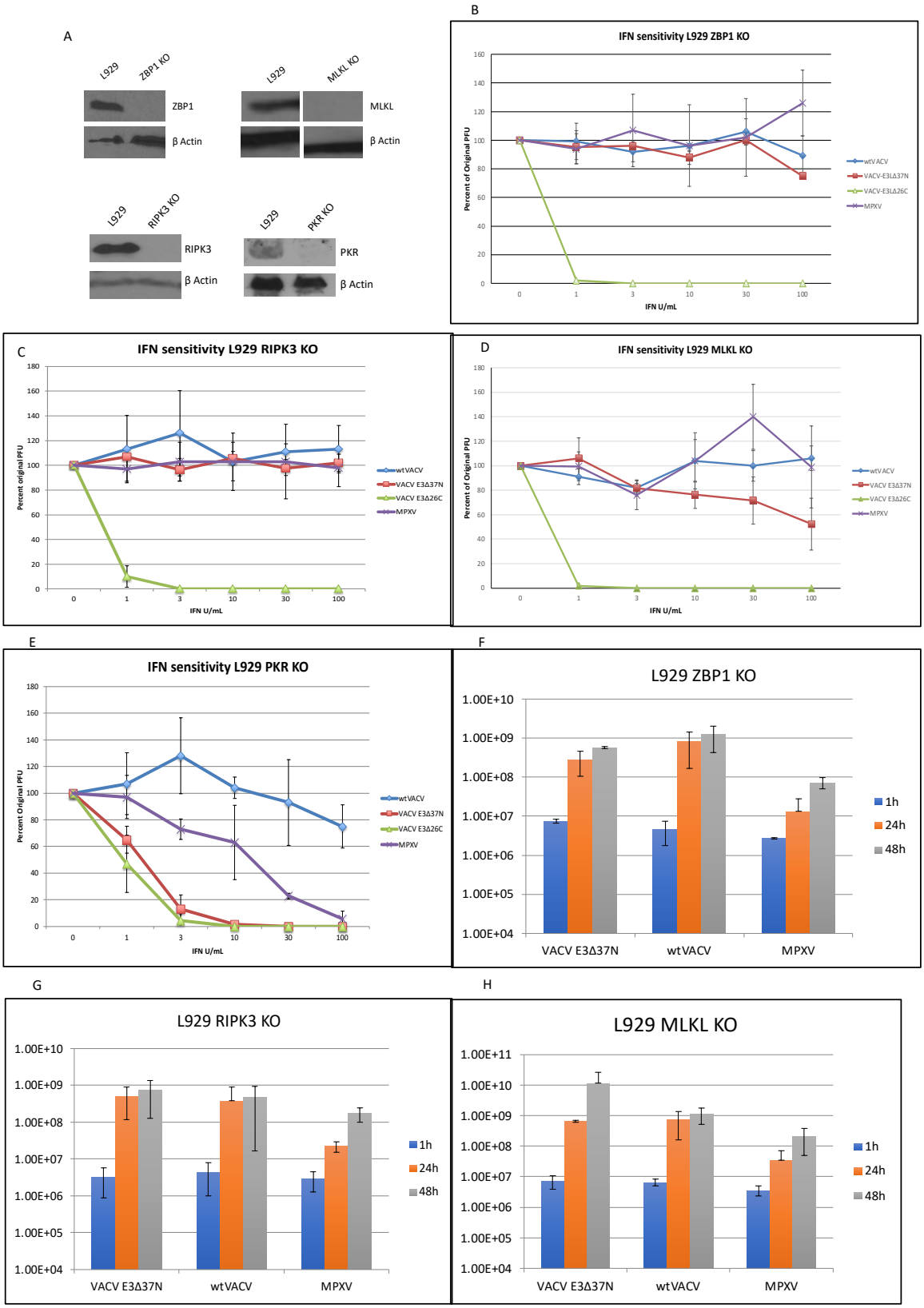
A
L929
ZBP1 KO
ZBP1
β Actin
L929
MLKL KO
MLKL
β Actin
L929
RIPK3 KO
RIPK3
β Actin
L929
PKR KO
PKR
β Actin
B
IFN sensitivity L929 ZBP1 KO
Percent of Original PFU
IFN U/mL
wtVACV
VACV-E3LΔ37N
VACV-E3LΔ26C
MPXV
C
IFN sensitivity L929 RIPK3 KO
Percent original PFU
IFN U/mL
wtVACV
VACV E3Δ37N
VACV E3Δ26C
MPXV
D
IFN sensitivity L929 MLKL KO
Percent of Original PFU
IFN U/mL
wtVACV
VACV E3Δ37N
VACV E3Δ26C
MPXV
E
IFN sensitivity L929 PKR KO
Percent Original PFU
IFN U/mL
wtVACV
VACV E3Δ37N
VACV E3Δ26C
MPXV
F
L929 ZBP1 KO
1h
24h
48h
VACV E3Δ37N
wtVACV
MPXV
G
L929 RIPK3 KO
1h
24h
48h
VACV E3Δ37N
wtVACV
MPXV
H
L929 MLKL KO
1h
24h
48h
VACV E3Δ37N
wtVACV
MPXV

Figure 2.2. IFN sensitivity is dependent on ZPB1, RIPK3, and MLKL but not PKR. A) Western blot confirming CRISPR KO L929 cells. B-E) IFN plaque reduction assays with CRISPR ZBP1, RIPK3, MLKL, and PKR KO L929 cells. F-H) 1-step viral growth curves in ZBP1, RIPK3, and MLKL KO L929 cells. Cells were pretreated with 100 U IFNα and infected with wtVACV, VACV- E3Δ37N, or MPXV at an MOI of 5. Viral titers were determined by plaquing in BSC40 cells.

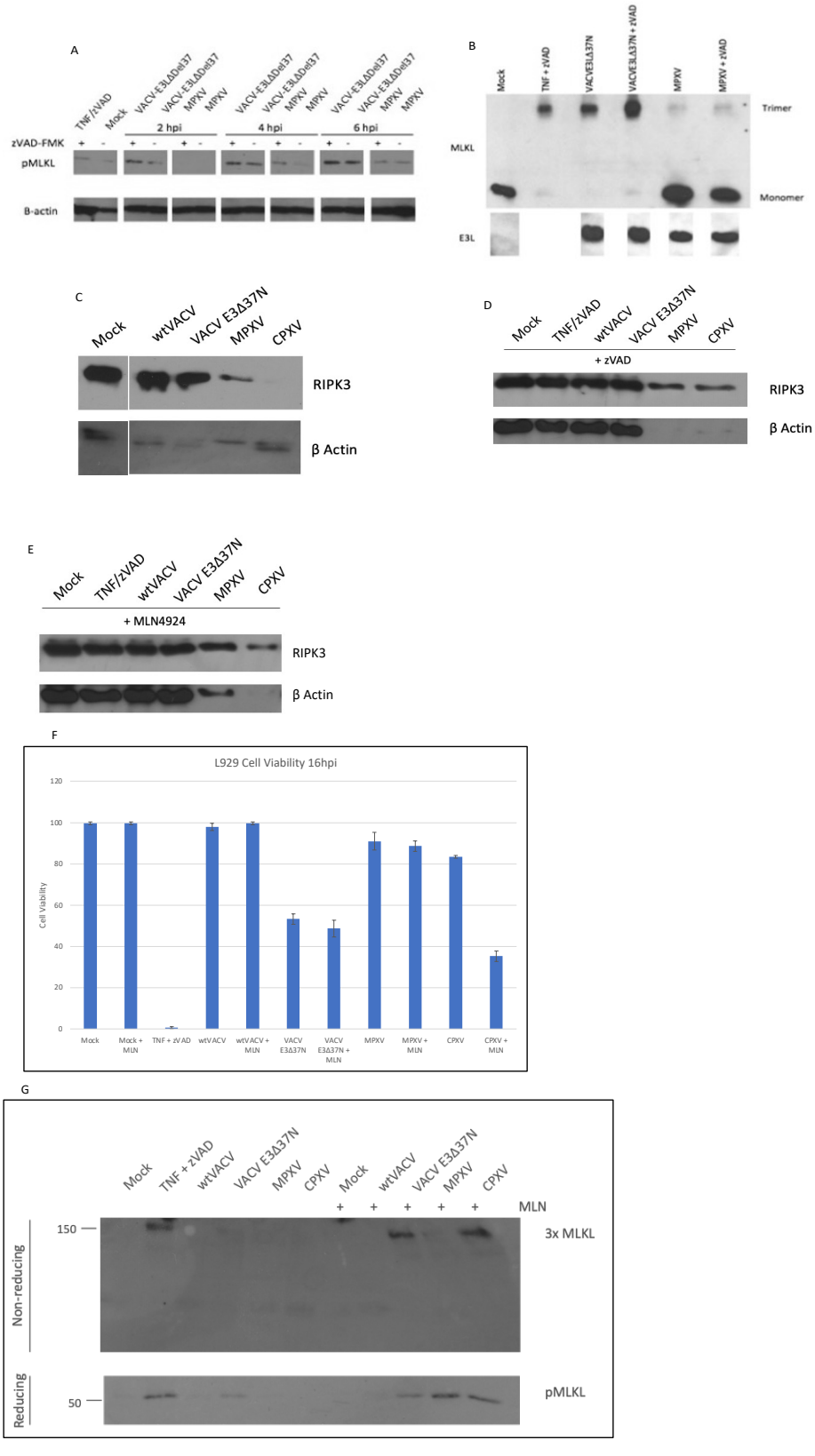
A
TNF/zVAD
Mock
VACV-E3LΔDel37
VACV-E3LΔDel37
MPXV
MPXV
2 hpi
4 hpi
6 hpi
zVAD-FMK
pMLKL
B-actin
B
Mock
TNF + zVAD
VACVE3LΔ37N
VACVE3LΔ37N + zVAD
MPXV
MPXV + zVAD
MLKL
Trimer
Monomer
E3L
C
Mock
wtVACV
VACV E3Δ37N
MPXV
CPXV
RIPK3
β Actin
D
Mock
TNF/zVAD
wtVACV
VACV E3Δ37N
MPXV
CPXV
+ zVAD
RIPK3
β Actin
E
Mock
TNF/zVAD
wtVACV
VACV E3Δ37N
MPXV
CPXV
+ MLN4924
RIPK3
β Actin
F
L929 Cell Viability 16hpi
Cell Viability
120
100
80
60
40
20
0
Mock
Mock + MLN
TNF + zV AD
wtV ACV
wtV ACV + MLN
VACV E3Δ37N
VACV E3Δ37N + MLN
MPXV
MPXV + MLN
CPXV
CPXV + MLN
G
Mock
TNF + zVAD
wtVACV
VACV E3Δ37N
MPXV
CPXV
Mock
wtVACV
VACV E3Δ37N
MPXV
CPXV
+ + + + +
MLN
150
3x MLKL
Non-reducing
Reducing
50
pMLKL

Figure 2.3. MPXV vIRD leads to RIPK3 cleavage and necroptosis inhibition. A) Western blot showing a time course of phosphorylated MLKL with and without zVAD. Viruses infected at an MOI of 5 and pretreated with 100 U IFNα. B) Western blot in non-reducing conditions for trimerized MLKL. C) Western blot showing RIPK3 degradation in MPXV and CPXV infected cells. D) Western blot for RIPK3 degradation with zVAD. E) Western blot for RIPK3 degradation with MLN4924. F) Cell viability assay with and without neddylation inhibitor, MLN4924. G) Western blot for phosphorylation and trimerization of MLKL with and without MLN4924.

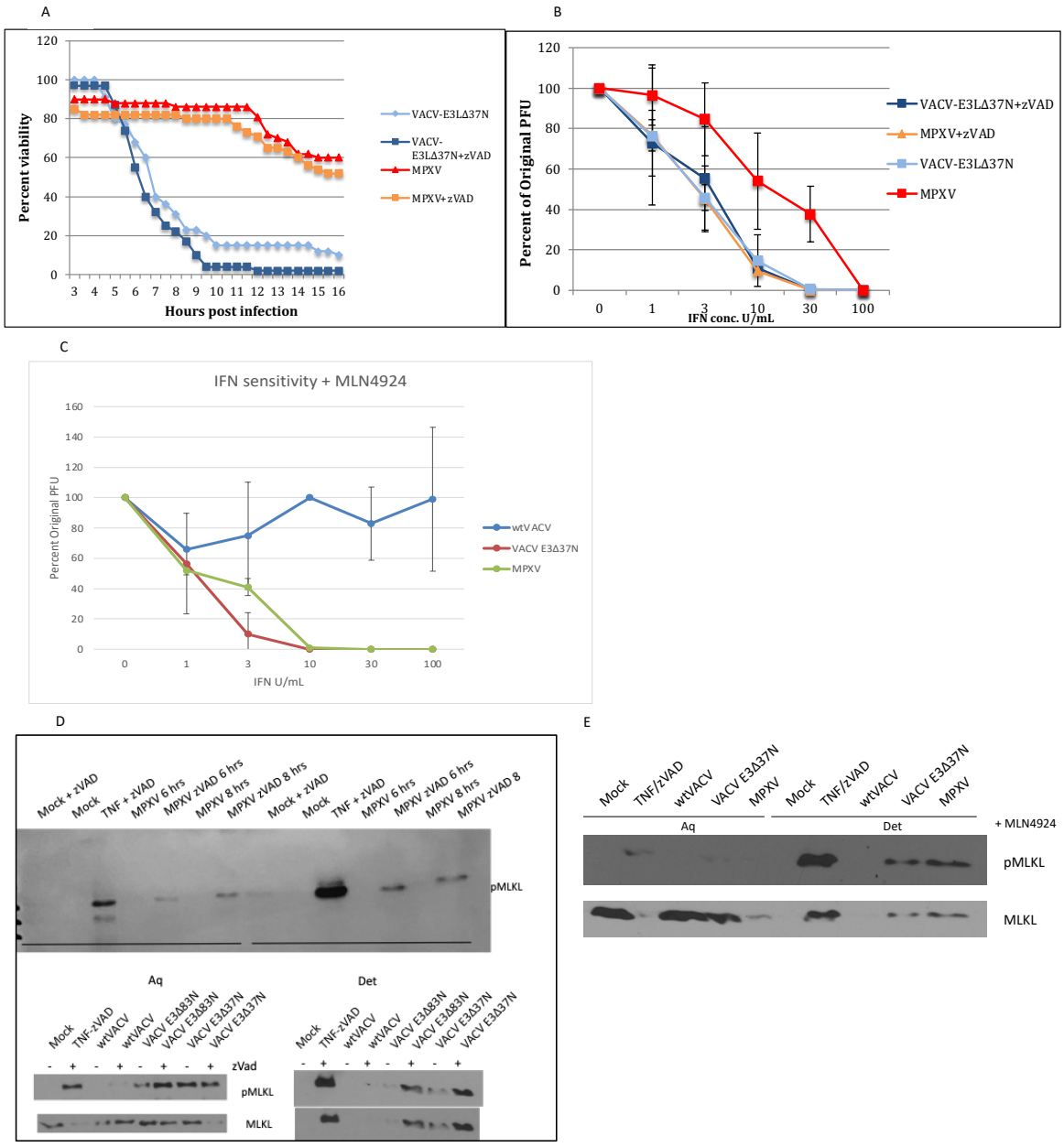

Figure 2.4. Caspase and neddylation inhibition leads to increased IFN sensitivity and MLKL membrane localization, but does not lead to necroptosis. A) SYTOX green cell viability assay with the addition of pancaspase inhibitor, zVAD. B) IFN plaque reduction assay with VACV-E3Δ37N and MPXV in the presence of zVAD. C) IFN plaque reduction assay with MLN4924. D) Western blot showing phosphorylation of MLKL localizing to membranes in the presence of zVAD. Viral samples were lysed with TX-114 allowing for separation. E) Same as D, but with MLN4924 instead of zVAD.

REFERENCES

[1] A. M. Likos *et al.*, "A tale of two clades: monkeypox viruses," *Journal of General Virology*, vol. 86, no. 10, pp. 2661–2672, doi: 10.1099/vir.0.81215-0.

[2] A. W. Rimoin *et al.*, "Major increase in human monkeypox incidence 30 years after smallpox vaccination campaigns cease in the Democratic Republic of Congo," *PNAS*, vol. 107, no. 37, pp. 16262–16267, Sep. 2010, doi: 10.1073/pnas.1005769107.

[3] K. D. Reed *et al.*, "The detection of monkeypox in humans in the Western Hemisphere," *New England Journal of Medicine*, vol. 350, no. 4, pp. 342–350, 2004.

[4] N. Erez *et al.*, "Diagnosis of Imported Monkeypox, Israel, 2018 - Volume 25, Number 5—May 2019 - Emerging Infectious Diseases journal - CDC", doi: 10.3201/eid2505.190076.

[5] A. Vaughan *et al.*, "Human-to-Human Transmission of Monkeypox Virus, United Kingdom, October 2018 - Volume 26, Number 4—April 2020 - Emerging Infectious Diseases journal - CDC", doi: 10.3201/eid2604.191164.

[6] S. E. F. Yong *et al.*, "Imported Monkeypox, Singapore - Volume 26, Number 8—August 2020 - Emerging Infectious Diseases journal - CDC", doi: 10.3201/eid2608.191387.

[7] A. K. Rao, "Monkeypox in a Traveler Returning from Nigeria — Dallas, Texas, July 2021," *MMWR Morb Mortal Wkly Rep*, vol. 71, 2022, doi: 10.15585/mmwr.mm7114a1.

[8] "Multi-country outbreak of monkeypox, External situation report #1 - 6 July 2022." https://www.who.int/publications/m/item/multi-country-outbreak-of-monkeypox--external-situation-report--1---6-july-2022 (accessed Jul. 08, 2022).

[9] J. G. Rizk, G. Lippi, B. M. Henry, D. N. Forthal, and Y. Rizk, "Prevention and Treatment of Monkeypox," *Drugs*, vol. 82, no. 9, pp. 957–963, Jun. 2022, doi: 10.1007/s40265-022-01742-y.

[10] G. Yang *et al.*, "An Orally Bioavailable Antipoxvirus Compound (ST-246) Inhibits Extracellular Virus Formation and Protects Mice from Lethal Orthopoxvirus Challenge," *J Virol*, vol. 79, no. 20, pp. 13139–13149, Oct. 2005, doi: 10.1128/JVI.79.20.13139-13149.2005.

[11] H.-W. Chang, J. C. Watson, and B. L. Jacobs, "The E3L gene of vaccinia virus encodes an inhibitor of the interferon-induced, double-stranded RNA-dependent

protein kinase," *Proceedings of the National Academy of Sciences*, vol. 89, no. 11, pp. 4825–4829, 1992.

[12] H.-W. Chang and B. L. Jacobs, "Identification of a conserved motif that is necessary for binding of the vaccinia virus E3L gene products to double-stranded RNA," *Virology*, vol. 194, no. 2, pp. 537–547, 1993.

[13] H.-W. Chang, L. H. Uribe, and B. L. Jacobs, "Rescue of vaccinia virus lacking the E3L gene by mutants of E3L.," *Journal of virology*, vol. 69, no. 10, pp. 6605–6608, 1995.

[14] H. Yuwen, J. H. Cox, J. W. Yewdell, J. R. Bennink, and B. Moss, "Nuclear localization of a double-stranded RNA-binding protein encoded by the vaccinia virus E3L gene," *Virology*, vol. 195, no. 2, pp. 732–744, 1993.

[15] J. C. Watson, H.-W. Chang, and B. L. Jacobs, "Characterization of a vaccinia virus-encoded double-stranded RNA-binding protein that may be involved in inhibition of the double-stranded RNA-dependent protein kinase," *Virology*, vol. 185, no. 1, pp. 206–216, 1991.

[16] T. A. Brandt and B. L. Jacobs, "Both carboxy-and amino-terminal domains of the vaccinia virus interferon resistance gene, E3L, are required for pathogenesis in a mouse model," *Journal of virology*, vol. 75, no. 2, pp. 850–856, 2001.

[17] W. D. Arndt *et al.*, "Evasion of the Innate Immune Type I Interferon System by Monkeypox Virus," *Journal of Virology*, vol. 89, no. 20, pp. 10489–10499, Oct. 2015, doi: 10.1128/JVI.00304-15.

[18] Y. Lin, A. Devin, Y. Rodriguez, and Z. Liu, "Cleavage of the death domain kinase RIP by Caspase-8 prompts TNF-induced apoptosis," *Genes Dev.*, vol. 13, no. 19, pp. 2514–2526, Oct. 1999.

[19] Y. Cho *et al.*, "Phosphorylation-Driven Assembly of the RIP1-RIP3 Complex Regulates Programmed Necrosis and Virus-Induced Inflammation," *Cell*, vol. 137, no. 6, pp. 1112–1123, Jun. 2009, doi: 10.1016/j.cell.2009.05.037.

[20] L. Sun *et al.*, "Mixed Lineage Kinase Domain-like Protein Mediates Necrosis Signaling Downstream of RIP3 Kinase," *Cell*, vol. 148, no. 1, pp. 213–227, Jan. 2012, doi: 10.1016/j.cell.2011.11.031.

[21] Z. Cai *et al.*, "Plasma membrane translocation of trimerized MLKL protein is required for TNF-induced necroptosis," *Nature Cell Biology*, vol. 16, no. 1, pp. 55–65, Jan. 2014, doi: 10.1038/ncb2883.

[22] E. S. Mocarski, J. W. Upton, and W. J. Kaiser, "Viral infection and the evolution of caspase 8-regulated apoptotic and necrotic death pathways," *Nature Reviews Immunology*, vol. 12, no. 2, pp. 79–88, Feb. 2012, doi: 10.1038/nri3131.

[23] Y. Dondelinger *et al.*, "MLKL compromises plasma membrane integrity by binding to phosphatidylinositol phosphates," *Cell reports*, vol. 7, no. 4, pp. 971–981, 2014.

[24] H. Wang *et al.*, "Mixed Lineage Kinase Domain-like Protein MLKL Causes Necrotic Membrane Disruption upon Phosphorylation by RIP3," *Molecular Cell*, vol. 54, no. 1, pp. 133–146, Apr. 2014, doi: 10.1016/j.molcel.2014.03.003.

[25] J. W. Upton, W. J. Kaiser, and E. S. Mocarski, "DAI/ZBP1/DLM-1 Complexes with RIP3 to Mediate Virus-Induced Programmed Necrosis that Is Targeted by Murine Cytomegalovirus vIRA," *Cell Host & Microbe*, vol. 11, no. 3, pp. 290–297, Mar. 2012, doi: 10.1016/j.chom.2012.01.016.

[26] H. Koehler *et al.*, "Inhibition of DAI-dependent necroptosis by the Z-DNA binding domain of the vaccinia virus innate immune evasion protein, E3," *Proceedings of the National Academy of Sciences*, vol. 114, no. 43, pp. 11506–11511, 2017.

[27] H. Koehler *et al.*, "Vaccinia virus E3 prevents sensing of Z-RNA to block ZBP1-dependent necroptosis," *Cell Host & Microbe*, vol. 29, no. 8, pp. 1266-1276.e5, Aug. 2021, doi: 10.1016/j.chom.2021.05.009.

[28] T. Shors, K. V. Kibler, K. B. Perkins, R. Seidler-Wulff, M. P. Banaszak, and B. L. Jacobs, "Complementation of Vaccinia Virus Deleted of the E3L Gene by Mutants of E3L," *Virology*, vol. 239, no. 2, pp. 269–276, Dec. 1997, doi: 10.1006/viro.1997.8881.

[29] S. Feng *et al.*, "Cleavage of RIP3 inactivates its caspase-independent apoptosis pathway by removal of kinase domain," *Cellular Signalling*, vol. 19, no. 10, pp. 2056–2067, Oct. 2007, doi: 10.1016/j.cellsig.2007.05.016.

[30] S. Alvarez-Diaz *et al.*, "The Pseudokinase MLKL and the Kinase RIPK3 Have Distinct Roles in Autoimmune Disease Caused by Loss of Death-Receptor-Induced Apoptosis," *Immunity*, vol. 45, no. 3, pp. 513–526, Sep. 2016, doi: 10.1016/j.immuni.2016.07.016.

[31] W. J. Kaiser *et al.*, "RIP3 mediates the embryonic lethality of caspase-8-deficient mice," *Nature*, vol. 471, no. 7338, pp. 368–372, Mar. 2011, doi: 10.1038/nature09857.

[32] A. Oberst *et al.*, "Catalytic activity of the caspase-8–FLIPL complex inhibits RIPK3-dependent necrosis," *Nature*, vol. 471, no. 7338, pp. 363–367, 2011.

[33] Z. Liu *et al.*, "A class of viral inducer of degradation of the necroptosis adaptor RIPK3 regulates virus-induced inflammation," *Immunity*, vol. 54, no. 2, pp. 247-258.e7, Feb. 2021, doi: 10.1016/j.immuni.2020.11.020.

[34] Y. Taguchi and H. M. Schätzl, "Small-scale Triton X-114 Extraction of Hydrophobic Proteins," *Bio Protoc*, vol. 4, no. 11, p. e1139, Jun. 2014, doi: 10.21769/BioProtoc.1139.

[35] B. P. Daniels *et al.*, "RIPK3 Restricts Viral Pathogenesis via Cell Death-Independent Neuroinflammation," *Cell*, vol. 169, no. 2, pp. 301-313.e11, Apr. 2017, doi: 10.1016/j.cell.2017.03.011.

[36] B. P. Daniels *et al.*, "The Nucleotide Sensor ZBP1 and Kinase RIPK3 Induce the Enzyme IRG1 to Promote an Antiviral Metabolic State in Neurons," *Immunity*, vol. 50, no. 1, pp. 64-76.e4, Jan. 2019, doi: 10.1016/j.immuni.2018.11.017.

CHAPTER 3

NECROPTOSIS INHIBITION BY MONKEYPOX VIRUS AND PKR DEPENDENT NECROPTOSIS

ABSTRACT

The vaccinia virus (VACV) E3 protein is an important immune evasion protein that is highly conserved among orthopoxviruses, with the exception of Monkeypox virus (MPXV). MPXV has re-emerged as the most important orthopoxvirus infection of humans and despite being highly pathogenic, it contains a natural truncation at the N-terminus of its E3 homologue leading to the loss of the first 37 amino acids. VACV E3 has a N-terminus Z-form nucleic acid binding domain and a C-terminus double stranded RNA binding domain. Both domains are required for pathogenesis, interferon resistance, and PKR inhibition. The N-terminus of the E3 protein is also required for evasion of ZBP1 dependent necroptosis by sequestering Z-form RNA and inhibiting recognition by ZBP1. VACV mutant containing an N-terminal deletion (VACV-E3LΔ37N) does not replicate in JC cells and induces rapid necroptotic cell death dependent on ZBP1, which activates RIPK3 leading to phosphorylation and trimerization of the executioner of necroptosis, MLKL. Despite lacking part of the N-terminus of E3, MPXV does not induce cell death, but inhibits necroptosis, and replicates efficiently in JC cells. Inhibition of necroptosis is dependent on function of the MPXV vIRD (viral inhibitor of RIPK3 degradation) leading to RIPK3 degradation. Since VACV lacks a functional vIRD, its replication is inhibited in JC cells, in a ZBP1-, RIPK3- and MLKL-dependent

manner. Interestingly, CRISPR PKR KO cells rescued VACV-E3LΔ37N viral replication and cell viability, indicating a link between PKR and necroptosis.

INTRODUCTION

Since the eradication of smallpox in 1977, monkeypox virus (MPXV) has been considered the most important orthopoxvirus infection in humans. It was originally discovered in cynomolgus monkeys in 1958 [1], with the first infected human case confirmed in the Democratic Republic of Congo (DRC) in 1971 [2]. The smallpox vaccine, which eradicated the causative agent of smallpox, the variola virus, is effective against MPXV. However, since the eradication of variola, and the subsequent halt in smallpox vaccinations there has been a drastic increase in the number of MPXV cases in West and Central Africa [3]. Until recently, MPXV in Africa was limited to small outbreaks, presumably due to zoonotic spillover. The first reported cases of MPXV outside of Africa occurred in the USA in 2003, where 47 people ranging from ages 3-43 years tested positive for MPXV, all linking back to an ill prairie dog that was in contact with an infected rodent that was imported into the US [4]. In 2017, Nigeria has their largest outbreak with 424 suspected MPXV cases and 155 confirmed cases. Factors that caused the outbreak were: immunology naïve population, increased encroachment of the wildlife habitats, increased human consumption of rodents/wildlife animals, heavy rainfall that caused humans and wildlife to come into close contact, immunosuppression due to HIV co-infections, and a young population [5]. Between 2018-2021, there were several cases of MPXV spread to Israel, the UK, Singapore, and Dallas, TX (USA) by travelers who had visited Nigeria [6 – 9]. In May 2022, there was a confirmed case in the UK, and since then, there has been other unrelated confirmed cases around the world. According to the CDC, at the time of writing this manuscript, there has been 14,511 confirmed cases of MPXV in 64 countries around the world [10].

Vaccinia virus (VACV) has become the model virus for studying orthopoxviruses. It is a large, double-stranded DNA virus that replicates in the cytoplasm of infected cells. VACV contains many ways to evade the host immune response and a crucial protein for evasion is the E3 protein. The E3 protein contains two conserved domains: the N-terminal Z-form nucleic acid (Z-NA) binding domain (ZBD) and the C-terminal dsRNA-binding domain (dsRBD). The C-terminal dsRBD is necessary for pathogenesis in mice [11 – 12], and replication in the majority of cells in culture [13]. It also sequesters double stranded RNA (dsRNA) to avoid recognition from dsRNA-dependent pattern recognition receptors (PRRs), such as protein kinase R (PKR) and the 2', 5'-oligoadenylate synthetase (OAS) pathway [13 – 17]. The N-terminus is also necessary for mouse pathogenesis [11 – 12], but it is dispensable for replication and IFN resistance in many cell culture settings, with the exception of 129 MEFs [18], L929s [19], and JC cells [20]. The N-terminus is also required to fully inhibit PKR in 129 MEFs, HeLa cells, and in the murine model [18], [21].

During the VACV life cycle, dsRNA is made as a biproduct of post-replicative transcription. At intermediate and late times post infection VACV transcripts do not contain precise termination sequences, thus long run-on transcripts are formed, and if the transcripts are encoded on opposite strands of the DNA, the transcripts can hybridize and form dsRNA [22]. dsRNA is a potent pathogen-associated molecular pattern (PAMP), that can initiate innate immune responses by various pathways. These PAMPs can be recognized by PRRs, such as RIG-1, MDA5, and TLR3 and they can also initiate type I IFN production and stimulate the expression of interferon-stimulated genes (ISGs), such as PKR, ADAR, and oligoadenylate synthetase (OAS) [23].

Expression of the VACV E3L gene leads to formation of two proteins, one full-length protein that contains both N- and C- terminal domains (p25), and a smaller N-terminally truncated protein (p20) that results from leaky translation. The E3 homologue in MPXV, F3, contains a natural truncation at the N-terminus that causes the first 37 amino acids to be deleted, resembling p20 of VACV. A genomic comparison of the E3 homologue between MPXV and VACV showed that they are 92% identical at the nucleotide level [20]. In this paper, we examined how MPXV has evolved to inhibit innate immunity and remain pathogenic, despite the N-terminal truncation in its E3 homologue.

Necroptosis is a lytic and inflammatory form of cell death. It is caspase independent and dependent on RHIM-containing proteins: receptor-interacting protein kinase 1 (RIPK1), RIPK3, TIR-domain-containing adapter-inducing IFN-β (TRIF), or Z-DNA-binding protein 1 (ZBP1, also known as DAI or DLM1) [24 – 27]. RIPK3 is a protein kinase that interacts with other RHIM-containing proteins and phosphorylates MLKL, resulting in MLKL aggregation at the plasma membrane leading to loss of membrane integrity and cell death [28 – 29]. While PKR has been implicated in IFN-γ induced necroptosis of FADD or Caspase 8 -/- MEFs, it does not play a role in IFN-α induced necroptosis of L929 or macrophages [30 – 32]. PKR has never before been shown to be important for pathogen-induced necroptosis.

Cowpox virus (CPXV) contains a viral inducer of RIPK3 degradation (vIRD) that targets RIPK3 to the SKP1-Cullin1-F-box (SCF) machinery, leading to ubiquitination and proteasomal degradation of RIPK3, inhibiting necroptosis and allowing for virus proliferation [33]. Protein degradation is regulated by the ubiquitin system, which

regulates many key biological processes, such as cell homeostasis, transcriptional regulation, endocytosis, and signal transduction [34]. The F-box binds the protein substrate and recruits it to the SCF ubiquitin ligase machinery for degradation [35]. The vIRD protein contains six ankyrin repeats at the N-terminus and a C-terminal F-box, the first five ankyrin repeats being essential for RIPK3 binding [33]. Here, we examine the role of MPXV vIRD in necroptosis inhibition.

The VACV N-terminus of E3 is necessary to inhibit IFN-primed necroptosis and for IFN resistance in L929 cells. Interferon-treated L929 cells infected with VACV mutant viruses that are missing part or the entire Z-NA binding domain of the N-terminus (VACV- E3Δ37N or VACV- E3Δ83N) induce rapid cell death that is ZBP1- and RIPK3-dependent [19]. ZBP1 and E3 compete for cytoplasmic Z-RNA that is made during VACV infection. If WT E3 is present, it will sequester the Z-RNA preventing ZBP1 recognition and inhibiting necroptosis. If E3 is missing the Z-NA binding domain, ZBP1 will recognize the Z-RNA and active necroptosis [36]. In this manuscript, we show that necrosome formation in JC cells requires PKR sensing of dsRNA. Furthermore, we have demonstrated that MPXV evades necroptosis and proliferates in JC cells by making less dsRNA, and thus not activating PKR, which is necessary for induction of necroptosis in JC cells, and by degrading RIPK3 in a proteosome-dependent manner, providing insights into MPXV evolution.

MATERIALS AND METHODS

Cell lines and treatments. The JC cells and all the JC KO cells was maintained with Roswell Park Memorial Institute medium (RPMI), supplemented with 10% heat inactivated FBS. All cell lines were incubated at 37℃ and supplemented with 5% CO_2. FBS was heat-inactivated by incubation at 56℃ for 30 minutes. BSC40 cells were maintained in Dulbecco's Modified-Minimal Essential Medium (DMEM) supplemented with 5% FBS. HeLa cells were maintained in DMEM supplemented with 5% FBS, 1X NEAA, and 200 μM L-glutamine. For TNF-induced necroptosis, cells were pretreated with the pancaspase inhibitor zVAD-FMK (ApexBio) at 50 μM for 1 hour followed by TNF-α (Sigma) at 20 ng/mL. Necroptosis was inhibited using RIPK1 and RIPK3 inhibitors, GSK 963 and GSK 872, at 10 μM concentration for 1 hour prior to and after infection. Inhibition of RIPK3 cleavage was accomplished using neddylation inhibitor MLN4924 (ApexBio) at 5 μM for 1 hour prior to and after infection. In order to increase the amount of dsRNA made by VACV and to select for low dsRNA producing viruses, IBT was used as previously described [38 – 39].

Viruses. For all VACV WT infections, Western Reserve (WR) strain was used. The N-terminus E3 mutant, VACV-E3Δ37N, was constructed as previously described [40]. The low dsRNA VACV-E3Δ37N mutants were generated by plaque picking in the presence of IBT. The E3 WT mutant with low dsRNA, VACV mutA24R virus, was a gift from Richard Condit's lab [38 – 39]. For all MPXV infections, WR 7-61 of the Western African strain was used in accordance with the protocols approved by Arizona State University and the CDC.

Cell viability assays. JC and JC KO cells were seeded on a 48-well CytoOne tissue culture-treated plates (USA Scientific) to be 80% on the day of infection. Cells were infected with the viruses of interest and incubated for 1 hour at 37℃ and rocked every 10 minutes. For nuclear staining, Hoechst 33342 was added to the media overlay along with 1 μM SYTOX green, or propidium iodine (PI), to stain for membrane integrity. The plate was then incubated at 37℃ with 5% CO_2 on an EVOS FL auto imaging microscope (Invitrogen) and images taken at the indicated time points. For CellTiter-Glo, cells were harvested at 18 hours post infection/treatment and measured using the manufacturer's protocol.

Growth kinetics. Cells were seeded in a 12-well plate to be 80% confluent on the day of infection. For single-step growth curves, MOI of 5 was used with the indicated viruses. After the 1-hour infection, cells were washed 3X with prewarmed media before adding the growth media overlay. The cells were then scraped and went through three freeze/thaw cycles before plaquing in BSC40s to determine viral titers. Multi-step growth curves were performed with the same protocol, except an MOI of 0.01 was used.

Protein extraction and Western blot analysis. Cells were seeded in a 12-well culture-treated plate to be 80% confluent on the day of infection. After infection, the cells were scraped into the media, pelleted, washed once with 1X PBS, and lysed in RIPA buffer (150 mM NaCl, 1% P-40, 0.5% sodium deoxycholate, 0.1% SDS, 25 mM Tris pH 7.4) with 1X Halt Protease and Phosphatase Inhibitor Cocktail (Thermo Scientific) and incubated on ice for 5 minutes. For phosphorylated MLKL, lysates were passed through QIAshredder columns (Qiagen). Proteins were separated on SDS/Page, transferred to a

nitrocellulose membrane with 10 mM 3-(cyclohexylamino)-1-propane sulfonic acid (CAPS), 20% methanol, pH 11 for 1 hour at 100V. For trimerized MLKL, the proteins were transferred for 3 hours at 70V and proteins run under non-reducing conditions. The membranes were then blocked in 3% bovine serum albumin (BSA), followed by primary and secondary antibodies. The antibodies used were: ZBP1 (Zippy-1, Adipogen), RIPK3 (ProSci), pMLKL (abcam), MLKL (Cell Signaling Technology), and PKR (Santa Cruz). The secondary antibodies were goat anti-rabbit IgG or goat anti-mouse IgG (Cell Signaling Technology) and visualized by chemiluminescence with either SuperSignal West Pico PLUS or Dura substrate (ThermoFisher).

JC CRISPR KO cell lines. The JC KO cell lines were generated using the CRISPR/Cas9 system (Horizon Discovery). JC cells were transduced using Edit-R Lentiviral particles containing Cas9 sgRNA, followed by transduction with Edit-R Lentiviral sgRNA specific for ZBP1, RIPK3, PKR, and MLKL. The manufacturer's instructions were used for the protocol. Western blots were performed to confirm successful deletions.

RESULTS

The N-terminus of E3 in VACV is required for necroptosis evasion and for replication in JC cells. In infected mice, VACV- E3Δ37N and VACV- E3Δ83N were 1,000-fold less pathogenic compared to VACV WT after intracranial injection, demonstrating the necessity of the E3 N-terminus for pathogenesis *in vivo* [12]. Similarly, in JC cells (murine adenocarcinoma cells), N-terminal E3 deletion mutants fail to replicate compared to VACV WT or MPXV [20]. In L929 cells (murine fibroblasts) necroptosis drives cellular inhibition of VACV N-terminal E3 deletion mutants through Z-RNA recognition [19], [36]. Thus, we were interested to see if JC cells also inhibited growth of VACV N-terminal deletion mutants through necroptosis. Because not all cell types are capable of executing necroptosis, we first sought to determine if JC cells underwent cell death after chemical initiation of necroptosis. JC cells were stimulated with chemical inducers of necroptosis TNF/ZVD and necroptosis inhibitors GSK 872 (RIPK3) and GSK 961 (RIPK1) and assayed for mitochondrial activity at 18 hours post-treatment using CellTiter-Glo (Figure 3.1A). JC cells were susceptible to cell death that was recovered by using RIPK1 or RIPK3 inhibitors. JC cells died after treatment with the pancaspase inhibitor zVAD alone which is unusual because most cells require zVAD and TNF treatment for cell death. Next, we wanted to determine whether infected JC cells would also undergo necroptosis like L929 cells, so we either visualized infected cells hourly after infection using dye exclusion as a marker for cell permeability and death or harvested protein at 6 hours post infection and probed for phosphorylated MLKL a post-translational marker indicating activation of the executer of necroptosis. JC cells treated with TNF and zVAD began uptake of SYTOX green at 3 hours post-treatment with all

cells dead by 7 hours post-treatment and induced phosphorylation of MLKL (Fig. 3.1B and E). Infection with VACV WT did not lead to an increase in cell death nor phosphorylation of MLKL. The E3 N-terminus deletion mutant, VACV-E3Δ37N, killed 50% of cells by 10HPI and induced phosphorylation of MLKL. Inhibition of RIPK1 did not appreciably rescue cell viability, while RIPK3 inhibition fully rescued cell viability in cells infected with VACV- E3Δ37N, suggesting that these cells were undergoing necroptosis. Cells infected with MPXV did not undergo rapid cell death but showed a delayed phenotype with cell death levels more similar to VACV WT than to VACV-E3Δ37N. MPXV infected cells also did not show detectable levels of phosphorylated MLKL (Fig. 3.1B and E). These data show that the VACV N-terminus of E3 is required to inhibit necroptosis in JC cells, but that MPXV does not induce necroptosis despite missing a full length E3 N-terminus.

Viral replication in JC cells was investigated using single-step growth curves (MOI 5) and multi-step growth curves (MOI 0.01). We observed that VACV WT and MPXV replicate efficiently, while VACV- E3Δ37N does not (Fig. 3.1C and D). VACV WT replicated nearly 2-logs in infection with a high MOI and 3-logs with a low MOI, MPXV replicated approximately 2-logs with a high MOI and 1.5-logs with a low MOI, while VACV-E3Δ37N yielded no output virus with either MOI. To ensure that the MPXV F3 homologue did not have any unforeseen function, VACV ΔE3::MPXV F3 was used in the multi-step growth curve and did not yield significant virus (Fig. 3.1C) [20]. These data show that the N-terminus of E3 VACV is required for replication in JC cells and the F3 homologue in MPXV is not solely responsible for viral growth.

Low dsRNA not sufficient to recover growth. Both wtVACV and VACV-E3Δ37N produce high levels of dsRNA during infection, while there are no detectable levels of dsRNA with MPXV infection [37]. VACV- E3Δ37N and MPXV have equivalent E3 proteins, but different levels of dsRNA made during infection, so we created a mutant VACV- E3Δ37N that made similar levels of dsRNA as MPXV. This was done by plaquing VACV- E3Δ37N in the presence of 60 μM isatin β-thiosemicarbazone (IBT) in BSC40 cells. IBT is an anti-poxvirus drug that increases dsRNA production of intermediate/late transcripts by enhancing the VACV polymerase and leading to long mRNA transcripts [38]. This generated two low dsRNA IBT resistant VACV- E3Δ37N mutants, VACV- E3Δ37N IBTR3 and VACV- E3Δ37N IBTR7.

To ensure that VACV- E3Δ37N IBTR3 and VACV- E3Δ37N IBTR7 were fully IBT resistant due to low dsRNA and not due to lack of IBT exposure, levels of dsRNA were measured using a slot blot in the presence and absence of IBT (Fig. 3.2A). The levels of dsRNA were similar in both VACV WT and VACV- E3Δ37N with or without IBT, with 1-fold increase in dsRNA with addition of IBT. Cells infected with VACV-E3Δ37N IBTR3 or VACV- E3Δ37N IBTR7 had 2-fold less dsRNA compared to VACV-E3Δ37N and a slight increase when treated with IBT. VACV mutA24R, a known IBT resistant virus with low dsRNA, had dsRNA levels comparable to mock treated cells with only a half fold increase with the addition of IBT (Fig. 3.2B). This confirmed that the resistance to IBT in cells infected with VACV- E3Δ37N IBTR3 or VACV- E3Δ37N IBTR7 was due to less dsRNA being produced.

Next, we wanted to see if reducing the amount of dsRNA would rescue VACV-E3Δ37N viral growth in JC cells. We compared viral growth in the permissive cell line, BSC40s, and in JC cells infected with VACV WT, VACV- E3Δ37N, and VACV-E3Δ37N IBTR3 and IBTR7 at an MOI of 0.01. All viruses grew about 5-logs in BSC40s, but in JC cells, only VACV WT replicated (Fig. 3.2D) showing that VACV-E3Δ37N and low dsRNA viruses have the capacity to replicate in these cells. We then looked at viral replication at multiple time points with an MOI of 0.01 or 5 with the same viruses and the addition of MPXV and VACV mutA24R, a VACV that has a WT E3 but low dsRNA levels. In the single-step growth curve, VACV WT, VACV mut24R and MPXV grew 3-logs while VACV- E3Δ37N and VACV- E3Δ37N IBTR3 and IBTR7 failed to replicate (Fig. 3.2E). In the multi-step growth curve, VACV and VACV mutA24R grew 4-logs, MPXV grew 3-logs, and VACV- E3Δ37N along with VACV-E3Δ37N IBTR3 and IBTR7 viruses failed to grow (Fig. 3.2F). This demonstrates that low dsRNA is not sufficient to rescue VACV- E3Δ37N viral replication in JC cells.

Both reduction of dsRNA and inhibition of RIPK3 is required to recover growth of N-terminal deletion mutants. Cell death was investigated using the VACV low dsRNA mutants, VACV- E3Δ37N IBTR3 and IBTR7, to see if dsRNA played a role in necroptosis. At twelve hours post infection, mock and VACV WT had no significant amount of death as measured by dye-exclusion, while VACV-E3Δ37N had a 50% reduction in cell viability. VACV-E3Δ37N IBTR3 and IBTR7 had comparable levels of cell death to MPXV, approximately 75%, indicating that reducing the amount of dsRNA was sufficient to partially restore cell viability (Fig. 3.3B). Phosphorylation of MLKL was detected in TNF/zVAD treatment and in VACV E3 N-terminal deletion mutants with

normal dsRNA levels, but not in VACV-E3Δ37N IBTR3, VACV-E3Δ37N IBTR7, or MPXV infections (Fig. 3.3C). Inhibition of RIPK3 kinase activity was required to fully inhibit necroptosis with all virus infections. The lack of phosphorylated MLKL with VACV- E3Δ37N IBTR viruses signifies that unlike L929 cells [36], in JC cells low dsRNA is sufficient to inhibit necroptosis.

Viral growth was examined using MPXV, VACV, VACV- E3Δ37N and VACV low dsRNA viruses with and without a RIPK3 inhibitor. In a single-step growth curve, VACV-E3Δ37N, VACV-E3Δ37N IBTR3 and IBTR7 viruses had reduced or no virus output at 24 hours post infection, with VACV WT and MPXV replicating more than 10-fold. Addition of the RIPK3 kinase inhibitor, GSK 872, had no effect on virus production in VACV WT or MPXV infection compared to non-treated infections. In VACV-E3Δ37N infection, RIPK3 inhibition allowed for a slight increase in virus production, but viral output was increased 1 to 1.5 logs in VACV-E3Δ37N IBTR3 and IBTR7 infections (Fig. 3.3D). These data demonstrate that although low dsRNA is sufficient to inhibit necroptosis, it is not enough to recover viral growth, RIPK3 inhibition is also necessary.

PKR is necessary for VACV-E3Δ37N mediated necroptosis. Since our data suggested that both dsRNA signaling and RIPK3 kinase activity were necessary for induction of necroptosis and inhibition of replication of VACV- E3Δ37N, we wanted to examine what effect deletion of necroptosis proteins would have on VACV- E3Δ37N viral replication. JC cells were transduced with lentiviral Cas9 particles followed by transduction with a predesigned lentiviral sgRNA (Horizon) to target PKR, ZBP1, RIPK3, or MLKL. The CRISPR-Cas9 KO cells were confirmed via western blot (Fig.

3.4A). To look at viral replication in these KO cells, the cells were infected with VACV WT, VACV-E3Δ37N, or MPXV at an MOI of 5 and harvested at the indicated time points. The viruses were then plaqued in a permissive cell line, BSC 40s, to determine viral titer. VACV-E3Δ37N grew to near wt levels in ZPB1, RIPK3, MLKL and PKR KO cells with statistical differences in the 48 hpi samples in RIPK3 and MLKL KO cells. KO of these genes only had minor effects on replication of wtVACV and MPXV (Fig. 3.4B-E). This demonstrates that the VACV-E3Δ37N growth restriction due to the N-terminal deletion can be overcome by deleting ZBP1, RIPK3, PKR, or MLKL.

Since, deleting PKR, ZBP1, RIPK3, or MLKL rescued viral replication, we wanted to see if we could also inhibit cell death in these cell lines. Cells were mock infected, treated with TNF and zVAD or infected with VACV WT, VACV-E3Δ37N, or MPXV at an MOI of 5 and cell viability was measured in a SYTOX green exclusion assay. Deletion of ZBP1 fully inhibited necroptosis with VACV-E3Δ37N infection, while the cell line remained sensitive to TNF-induced necroptosis. Infection with VACV WT and MPXV also yielded no necroptosis (Fig. 3.5A). Virus infection in RIPK3 or MKLK KO cells gave no necroptosis and deleting these key necroptotic proteins also prevented TNF-induced cell death (Fig. 3.5B-C). In JC cells, VACV WT and MPXV gave no death while VACV-E3Δ37N and TNF/zVAD treated cells induced necroptosis (Fig. 3.5E). Phosphorylated and trimerized MLKL was only detected in cells treated with TNF/zVAD in ZBP1 KO cells and not in RIPK3 KOs, signifying that deletion of RIPK3 abolishes viral and TNF-induced necroptosis (Fig. 3.5F). PKR KO cells were still sensitive to TNF-induced cell death, but deleting PKR also inhibited VACV-E3Δ37N induced necroptosis (Fig. 3.5D). A western blot was performed to verify necroptosis by

probing for MLKL phosphorylation and trimerization in PKR KO cells. Only in TNF/zVAD treated cells did we detect phosphorylated and trimerized MLKL and none with VACV WT, VACV-E3Δ37N, or MPXV infected cells. We confirmed that the lack of necroptosis in PKR KOs was not due to insufficient virus infection by probing for VACV E3 protein (Fig. 3.5G). This data demonstrates that PKR is an important component of viral induced necroptosis in JC cells.

MPXV contains a viral inducer of RIPK3 degradation (vIRD) and leads to RIPK3 degradation and necroptosis inhibition. We wanted to see if MPXV contained a CPXV homologue that was leading to RIPK3 degradation and necroptosis inhibition. A vIRD protein sequence alignment was performed with VACV WT (Western Reserve), CPXV, and MPXV to check for sequence homology between the viruses. VACV WT contains the first and part of the second ankyrin repeat but is missing ankyrin repeats 3-6 and the F-Box. CPXV and MPXV share high sequence similarity throughout all the ankyrin repeats and the F-box (Fig. 3.6A). Next, we looked at RIPK3 expression in JC cells infected with VACV WT, VACV- E3Δ37N, MPXV, or CPXV and protein levels were analyzed 8 hours post infection via western blot. Cells infected with VACV WT or VACV- E3Δ37N expressed RIPK3 levels comparable to mock infected cells. Unsurprising, because the vIRD orthologue in VACV Western Reserve is missing the majority of the ankyrin repeats and the F-Box. Cells infected with CPXV had no detectable RIPK3 and MPXV infected cells had greatly reduced levels of RIPK3 expression (Fig. 3.6B). Since CPXV vIRD can target RIPK3 to the SCF machinery, leading to RIPK3 ubiquitination and degradation, CUL1 was chemically inhibited using neddylation inhibitor MLN4924 to prevent RIPK3 ubiquitination (Fig. 3.6C) and cell

viability was measured at 8 hours post infection using a SYTOX green exclusion assay. Addition of MLN4924 had no effect on mock treated cells or in VACV infected cells. Cells infected with VACV WT or VACV-E3Δ37N had no decrease in viability with the addition of MLN4924 compared to infected cells. MPXV and CPXV infection did not induce cell death in untreated cells, but MPXV infection with MLN4924 killed 50% of cells and CPXV infected cells with MLN4924 killed ~85% of infected cells (Fig. 3.6D). Initial data confirms that MPXV and CPXV induce necroptosis as visualized by western blot probing for phosphorylated and trimerized MLKL (observation). Neddylation inhibitor, MLN4924, effectively inhibited MPXV replication in a single-step growth curve (MOI 5) and restricted VACV-WT replication to less than a log (Fig. 3.6E). These data show that MPXV cleaves RIPK3 to inhibit necroptosis and to increase viral replication in JC cells. MLN4924 can efficiently induce necroptosis in MPXV infected cells and can inhibit viral replication.

DISCUSSION

The host response to viral pathogens is multifaceted in that it activates many antiviral responses through transcriptional upregulation and also initiates post-transcriptional responses to shut down virus production, such as induction of cell death pathways. The pathways activated differ by infecting pathogen and can be specific to cell and organ type in *in vitro* systems. In L929 cells infected with VACV N-terminal deletion mutants, necroptosis is the main form of anti-viral regulation by sensing Z-RNA and inducing cell death [19]. In this chapter, we show that there is more than one mechanism controlling VACV-E3Δ37N viral replication in JC cells which serve as an additional model to what we expect to see in *in vivo* infections. JC cells also distinguish themselves from L929 cells by implicating PKR in the necroptosis pathway. While in L929 cells, ZBP1 is the only inducer of necroptosis of VACV E3 N-terminal deletion mutants, we demonstrated that dsRNA plays a role in inducing necroptosis in JC cells. Cell death in JCs can be recovered both by reducing dsRNA formed by virus (Fig. 3.3) and by knocking out PKR expression (Fig. 3.5). Previous research in L929 cells demonstrated that neither reduction of dsRNA by VACV-E3Δ37N nor down-regulation of PKR recovered cell death [19], [36]. ZBP1 and RIPK3 also play a critical role in inhibition of viral replication in JC cells by recognizing Z-form nucleic acid and inducing necroptosis, but PKR is also an important component.

Necroptosis can occur through interaction of RIPK3 with any RHIM containing RIPK3 activators, RIPK1 (acting downstream of death receptors), TRIF (acting downstream of TLR 3 or TLR4), or ZBP1 (after viral recognition). These will all lead to RIPK3 activation which will phosphorylate and activate MLKL leading to cell death.

Here, we show that PKR is necessary for VACV-E3Δ37N-mediated necroptosis. The low dsRNA produced with VACV-E3Δ37N IBTR3 and IBTR7 viruses was sufficient to rescue cell viability, but not viral replication, suggesting another pathway is also involved. When we added a RIPK3 inhibitor to the infections with the low dsRNA mutants, we were able to see viral replication. The importance of PKR in necroptosis and inhibition of viral replication was confirmed with the PKR KO cells. Infection with VACV-E3Δ37N in PKR KOs did not induce necroptosis compared to wildtype JC cells and PKR KOs also rescued viral replication. Low dsRNA was sufficient to rescue cell viability, however RIPK3 was still activated, most likely by ZBP1 and/or PKR. RIPK3 was able to inhibit viral replication in a cell-death independent manner. This argues that low dsRNA and/or Z-RNA are the determining factor on which pathway the cell will take. The level of cell viability rescue with the low dsRNA viruses was only 70%, addition of RIPK3 inhibitor was required to reach 100% viability, arguing that it could be a combined effect of dsRNA and Z-RNA recognition. Additionally, RIPK3 has been shown to induce apoptosis in a FADD-dependent manner during influenza A virus (IAV) infection [39] and inhibit Zika virus (ZIKV) replication in a cell-independent manner [40]. Identifying the PAMP that is activating these pathways will be of high importance. Overall, our data show that PKR is required for necroptosis in JC cells. This is the first time that PKR has been implicated in pathogen-induced necroptosis.

The N-terminus of E3 has been shown to be important for viral replication *in vitro*, IFN resistance, PKR inhibition, and pathogenesis [11 – 12], [18], [20 – 21]. In JC cells, VACV-E3Δ37N infection leads to necroptosis and replication inhibition. MPXV has the same truncation in the N-terminus of E3 as in VACV-E3Δ37N but does not lead

to necroptosis or replication inhibition. It has been surprising that MPXV maintains its pathogenicity despite this truncation, thus MPXV has evolved ways in evading the host immune response. Firstly, MPXV makes less dsRNA than VACV and can thus evade PKR recognition [37]. In this paper, we show that MPXV has also evolved to inhibit necroptosis as we fail to see phosphorylation of MLKL or cell death with a viability assay. We demonstrate that MPXV inhibits necroptosis through a CPXV vIRD homologue which cleaves and leads to degradation of RIPK3, allowing for MPXV proliferation.

FIGURES

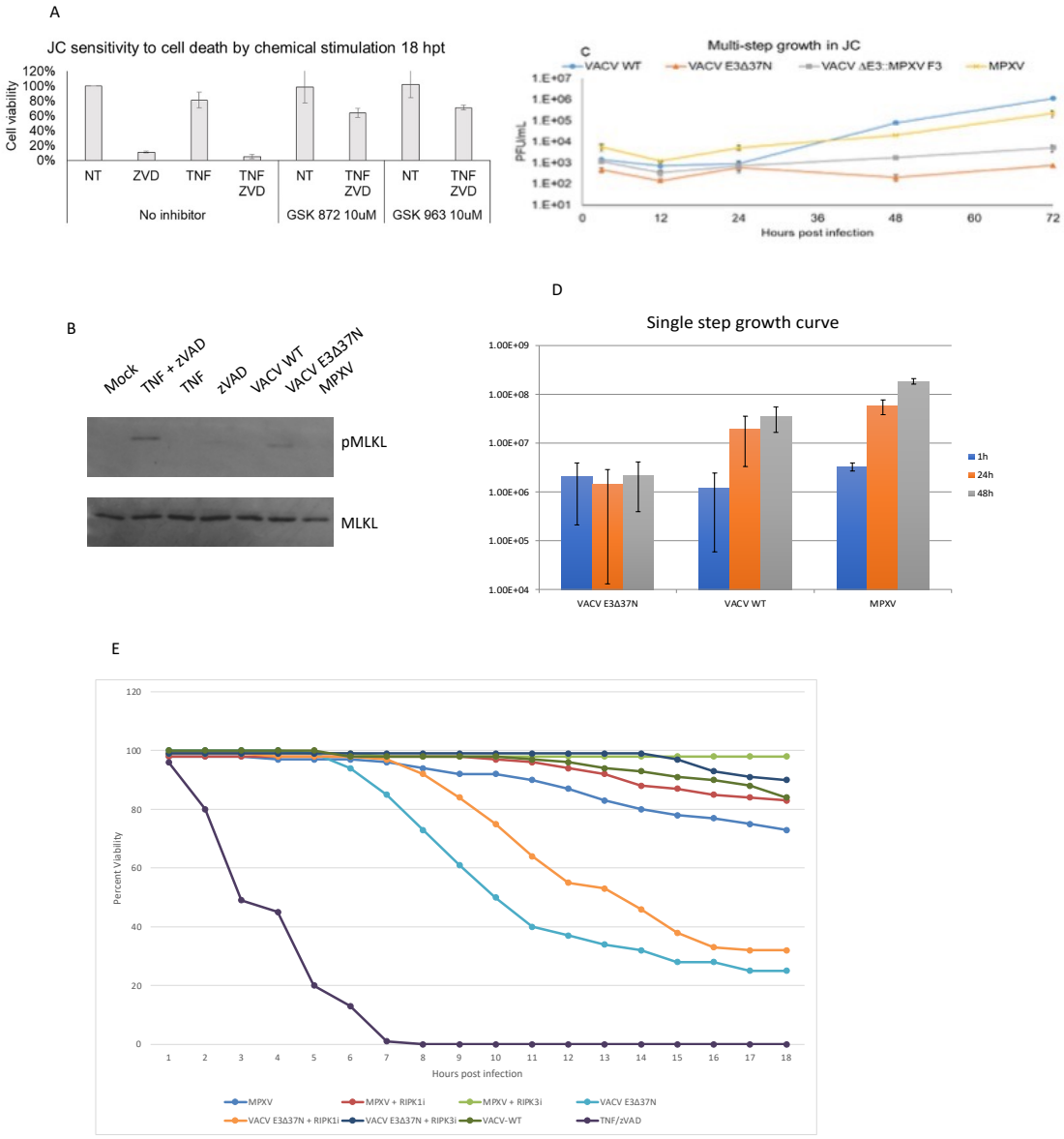

Figure 3.1. VACV-E3Δ37N induces necroptosis in JC cells. A) JC cells were infected with the indicated viruses at an MOI of 5 and a western blot was performed for phosphorylated MLKL. B). JC cells were infected/treated as indicated and cell viability was performed using Hoechst and SYTOX green for exclusion. Images were taken every hour with the EVOS FL auto imaging microscope. C) JC cells were infected with the indicated viruses at an MOI of 0.01, harvested at the indicated time points, and plaqued in BSC40 cells. D) JC cells were infected at an MOI of 5, harvested at the indicated time points, and plaqued in BSC40 cells.

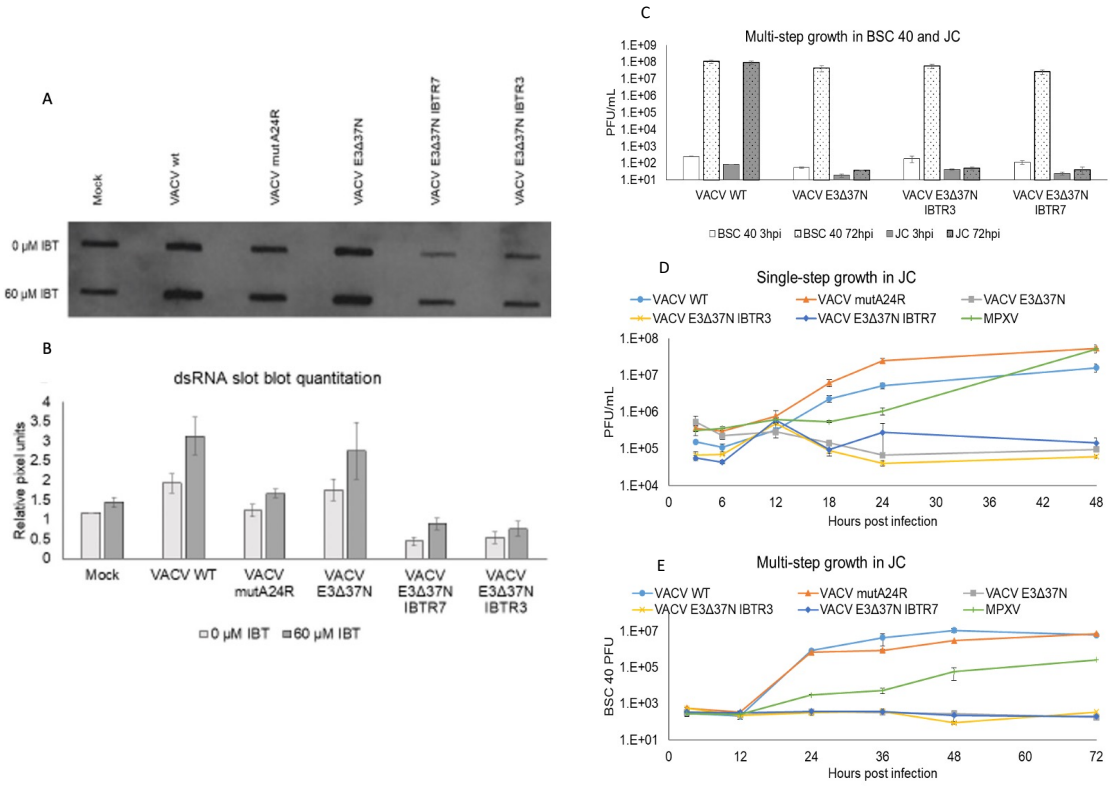

Figure 3.2. Low dsRNA is not sufficient to recover VACV-E3Δ37N growth. A) HeLa cells were infected at an MOI of 5 for 9 hours with the indicated viruses and the amount of dsRNA was determined using a slot blot. B) dsRNA bands were quantified using ImageJ. C) JC and BSC40 cells were infected at an MOI of 0.01 and harvested at 3 and 72 hours post infection. D) JC cells were infected at an MOI of 5, harvested at the indicated time points, and tittered in BSC40s. E) JC cells were infected at an MOI of 0.01, harvested at the indicated time points, and tittered in BSC40s.

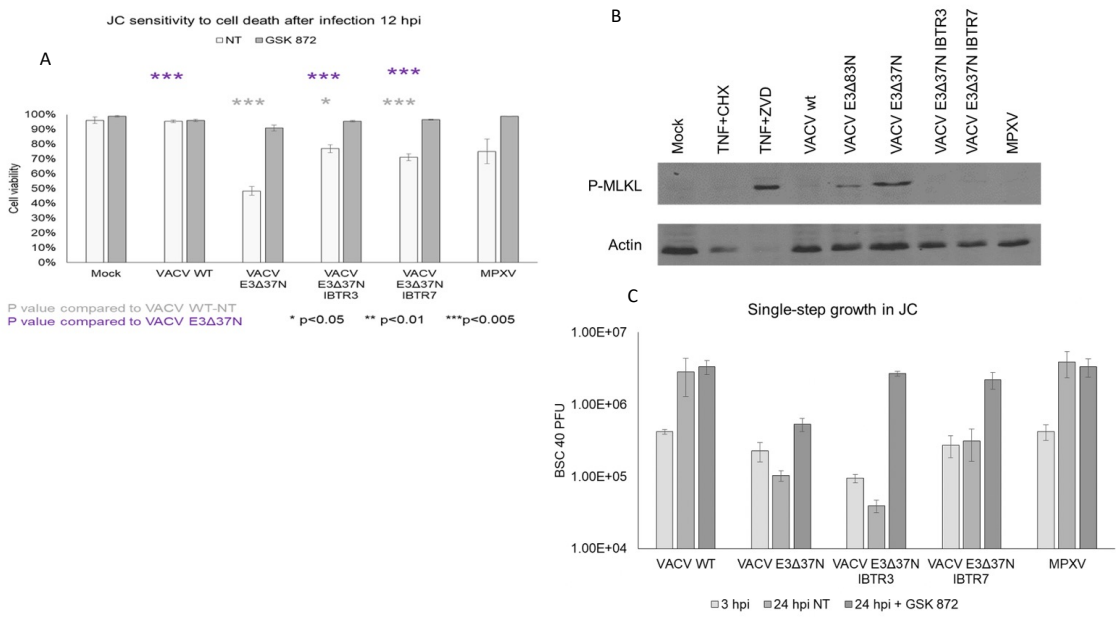

Figure 3.3. Low dsRNA rescues VACV-E3Δ37N cell viability, but RIPK3 inhibition is also required for replication in JC cells. A) JC cells were infected at an MOI of 5 and cell death was analyzed using Hoescht and PI exclusion at 12 hours post infection. B) Phosphorylation of MLKL was analyzed by western blot 12 hours after infection with the indicated viruses. C) JC cells were infected with the indicated viruses at an MOI of 5 with and without addition of RIPK3 inhibitor, GSK872. Cells were harvested and tittered in BSC40s.

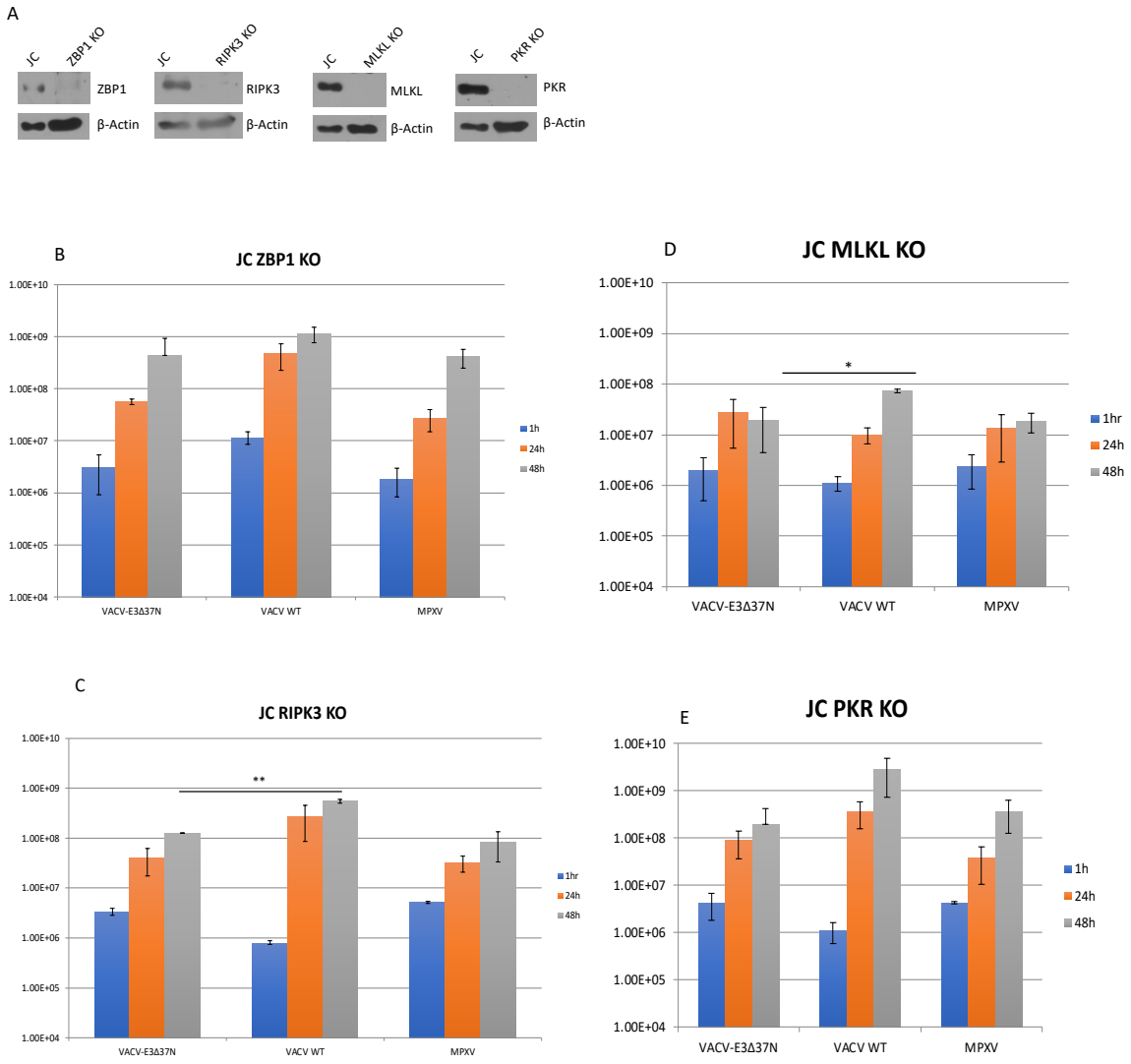

Figure 3.4. VACV-E3Δ37N replication is dependent on ZBP1, RIPK3, MLKL, and PKR. A) JC ZBP1, RIPK3, MLKL, and PKR KO cells confirmed via western blot. B-E) JC KO cells were infected with VACV-E3Δ37N, VACV WT, or MPXV at an MOI of 5, harvested at the indicated time points, and plaqued in BSC40 cells. *p=<.05, **p=<.01 when comparing VACV-E3Δ37N and VACV WT 48 hrs.

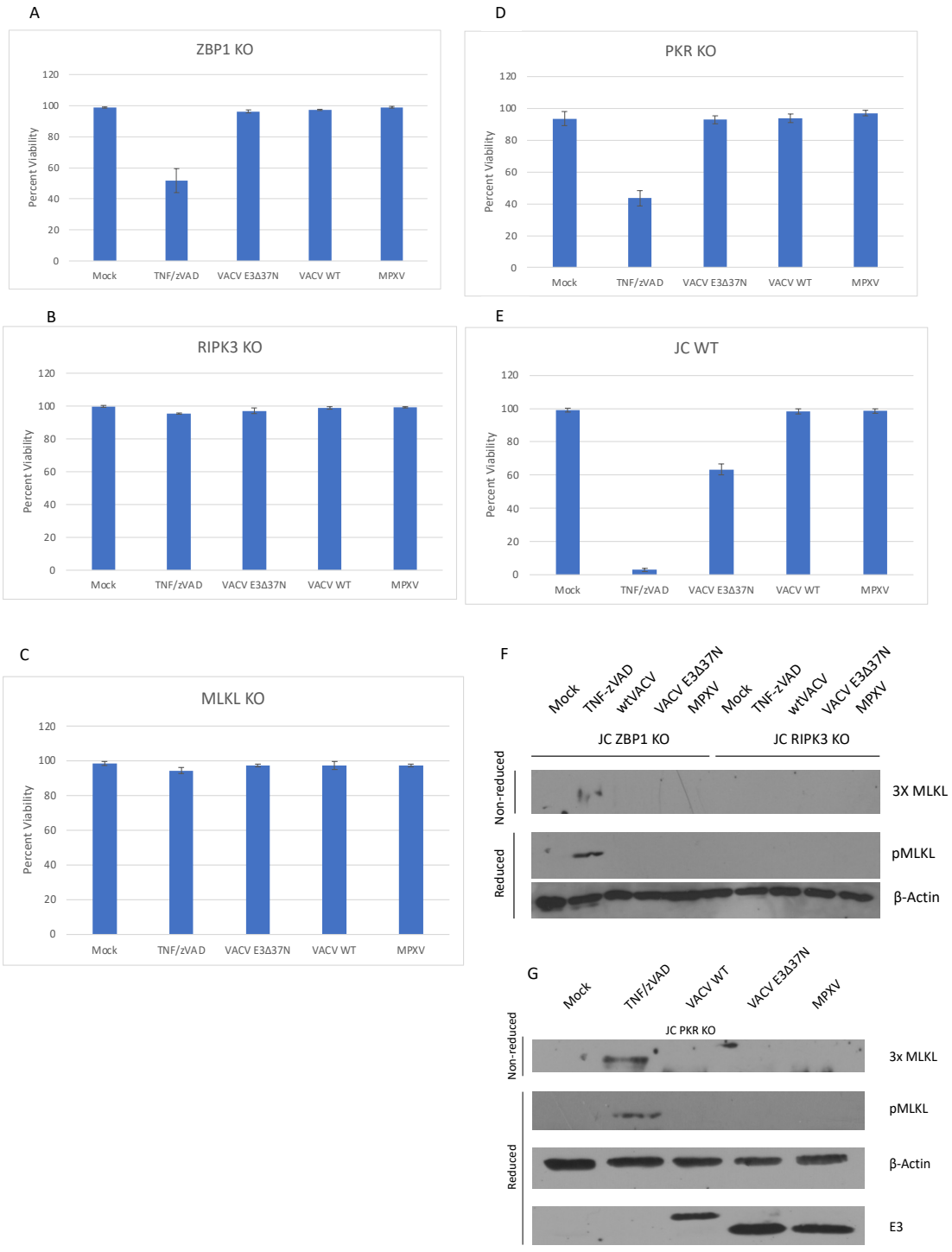

Figure 3.5. PKR is required for VACV-E3Δ37N-mediated necroptosis. (A-D), JC KO cells were infected at an MOI of 5 and cell viability was determined by Hoescht and SYTOX green exclusion on the EVOS FL auto imaging microscope. (E-F) Western blots

were performed to confirm necroptosis by probing for phosphorylated and trimerized MLKL.

A

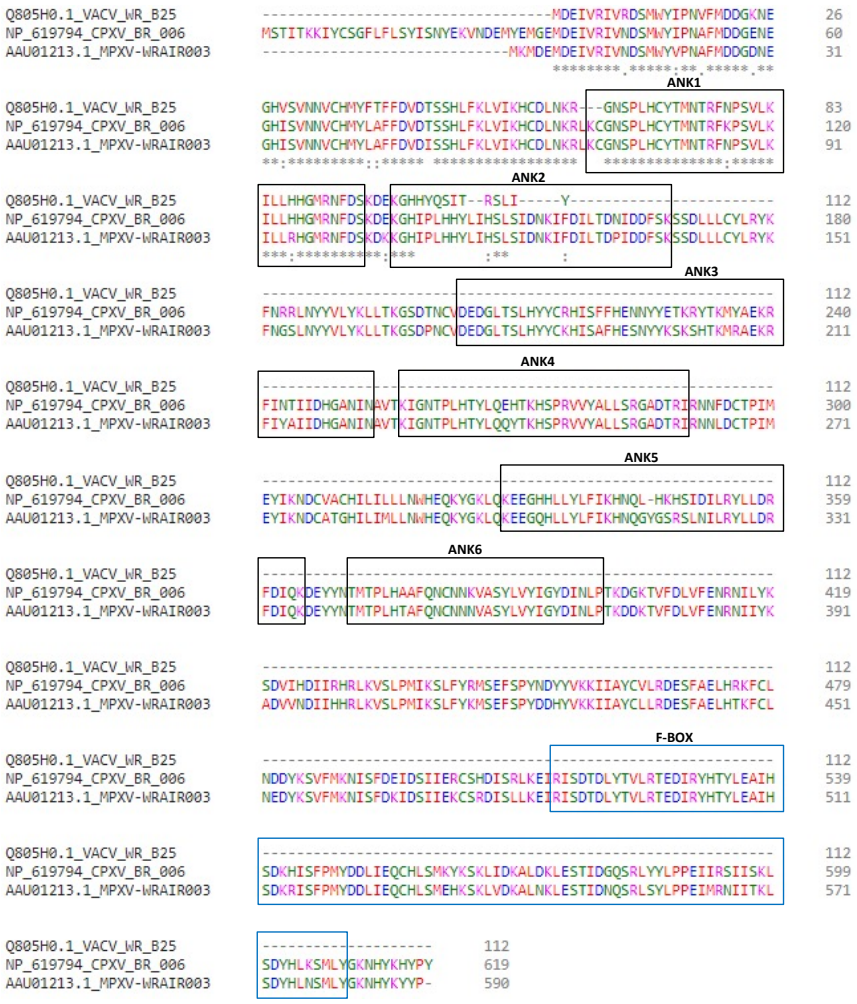
Q805H0.1_VACV_WR_B25
NP_619794_CPXV_BR_006
AAU01213.1_MPXV-WRAIR003
ANK1
ANK2
ANK3
ANK4
ANK5
ANK6
F-BOX

B

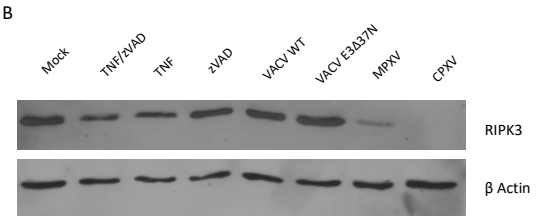
Mock
TNF/zVAD
TNF
zVAD
VACV WT
VACV E3Δ37N
MPXV
CPXV
RIPK3
β Actin

C

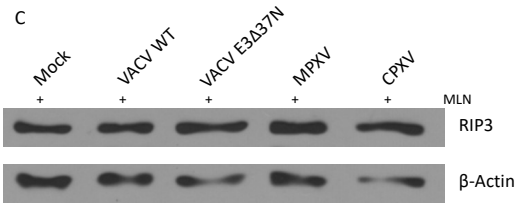
Mock
VACV WT
VACV E3Δ37N
MPXV
CPXV
MLN
RIP3
β-Actin

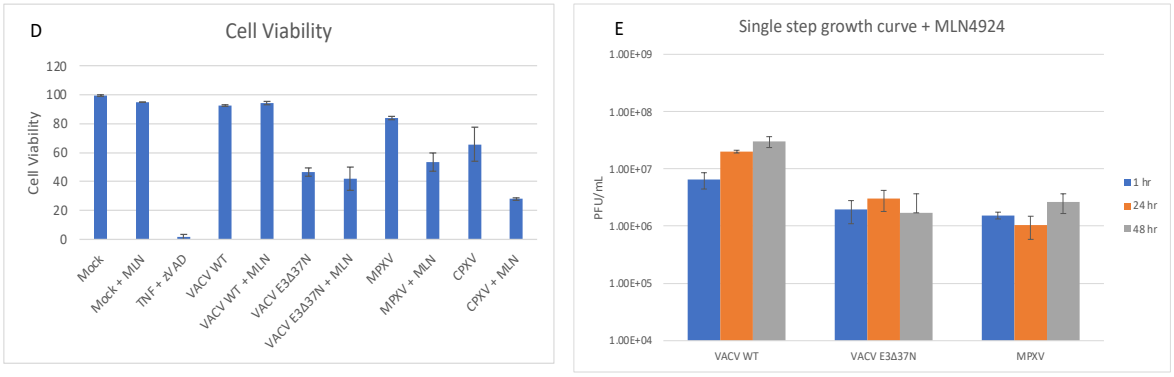

Figure 3.6. MPXV inhibits necroptosis by cleaving RIPK3. A) vIRD protein alignment with VACV WT, MPXV, and CPXV. Ankyrin repeats are shown in black boxes and the F-box in blue. Asterisks represent conserved amino acid residues. B) JC cells were infected at an MOI of 5 and 8 hours post infection RIPK3 levels were analyzed via western blot. C) JC cells were pretreated with neddylation inhibitor MLN4924 and infected as indicated, RIPK3 levels were analyzed 8 hours post infection via western blot. D) JC cells were infected at an MOI of 5 and cell viability was determined 8 hours post infection by Hoescht and SYTOX green exclusion on the EVOS FL auto imaging microscope. E) JC cells were pretreated with MLN4924 and infected with the indicated viruses at an MOI of 5 and viruses were tittered in BSC40 cells.

REFERENCES

[1] P. von Magnus, E. K. Andersen, K. B. Petersen, and A. Birch-Andersen, “A pox-like disease in cynomolgus monkeys,” *Acta Pathologica Microbiologica Scandinavica*, vol. 46, no. 2, pp. 156–176, 1959.

[2] I. D. Ladnyj, P. Ziegler, and E. Kima, “A human infection caused by monkeypox virus in Basankusu Territory, Democratic Republic of the Congo,” *Bull World Health Organ*, vol. 46, no. 5, pp. 593–597, 1972.

[3] A. W. Rimoin *et al.*, “Major increase in human monkeypox incidence 30 years after smallpox vaccination campaigns cease in the Democratic Republic of Congo,” *PNAS*, vol. 107, no. 37, pp. 16262–16267, Sep. 2010, doi: 10.1073/pnas.1005769107.

[4] K. D. Reed *et al.*, “The detection of monkeypox in humans in the Western Hemisphere,” *New England Journal of Medicine*, vol. 350, no. 4, pp. 342–350, 2004.

[5] E. Alakunle, U. Moens, G. Nchinda, and M. I. Okeke, “Monkeypox Virus in Nigeria: Infection Biology, Epidemiology, and Evolution,” *Viruses*, vol. 12, no. 11, Art. no. 11, Nov. 2020, doi: 10.3390/v12111257.

[6] N. Erez *et al.*, “Diagnosis of Imported Monkeypox, Israel, 2018 - Volume 25, Number 5—May 2019 - Emerging Infectious Diseases journal - CDC”, doi: 10.3201/eid2505.190076.

[7] A. Vaughan *et al.*, “Human-to-Human Transmission of Monkeypox Virus, United Kingdom, October 2018 - Volume 26, Number 4—April 2020 - Emerging Infectious Diseases journal - CDC”, doi: 10.3201/eid2604.191164.

[8] S. E. F. Yong *et al.*, “Imported Monkeypox, Singapore - Volume 26, Number 8—August 2020 - Emerging Infectious Diseases journal - CDC”, doi: 10.3201/eid2608.191387.

[9] A. K. Rao, “Monkeypox in a Traveler Returning from Nigeria — Dallas, Texas, July 2021,” *MMWR Morb Mortal Wkly Rep*, vol. 71, 2022, doi: 10.15585/mmwr.mm7114a1.

[10] “2022 Monkeypox Outbreak Global Map | Monkeypox | Poxvirus | CDC,” Jul. 20, 2022. https://www.cdc.gov/poxvirus/monkeypox/response/2022/world-map.html (accessed Jul. 20, 2022).

[11] T. A. Brandt and B. L. Jacobs, “Both carboxy-and amino-terminal domains of the vaccinia virus interferon resistance gene, E3L, are required for pathogenesis in a mouse model,” *Journal of virology*, vol. 75, no. 2, pp. 850–856, 2001.

[12] T. Brandt, M. C. Heck, S. Vijaysri, G. M. Jentarra, J. M. Cameron, and B. L. Jacobs, “The N-terminal domain of the vaccinia virus E3L-protein is required for neurovirulence, but not induction of a protective immune response,” *Virology*, vol. 333, no. 2, pp. 263–270, 2005.

[13] H.-W. Chang and B. L. Jacobs, “Identification of a conserved motif that is necessary for binding of the vaccinia virus E3L gene products to double-stranded RNA,” *Virology*, vol. 194, no. 2, pp. 537–547, 1993.

[14] H.-W. Chang, J. C. Watson, and B. L. Jacobs, “The E3L gene of vaccinia virus encodes an inhibitor of the interferon-induced, double-stranded RNA-dependent protein kinase,” *Proceedings of the National Academy of Sciences*, vol. 89, no. 11, pp. 4825–4829, 1992.

[15] H.-W. Chang, L. H. Uribe, and B. L. Jacobs, “Rescue of vaccinia virus lacking the E3L gene by mutants of E3L.,” *Journal of virology*, vol. 69, no. 10, pp. 6605–6608, 1995.

[16] H. Yuwen, J. H. Cox, J. W. Yewdell, J. R. Bennink, and B. Moss, “Nuclear localization of a double-stranded RNA-binding protein encoded by the vaccinia virus E3L gene,” *Virology*, vol. 195, no. 2, pp. 732–744, 1993.

[17] J. C. Watson, H.-W. Chang, and B. L. Jacobs, “Characterization of a vaccinia virus-encoded double-stranded RNA-binding protein that may be involved in inhibition of the double-stranded RNA-dependent protein kinase,” *Virology*, vol. 185, no. 1, pp. 206–216, 1991.

[18] S. D. White and B. L. Jacobs, “The amino terminus of the vaccinia virus E3 protein is necessary to inhibit the interferon response,” *Journal of virology*, vol. 86, no. 10, pp. 5895–5904, 2012.

[19] H. Koehler *et al.*, “Inhibition of DAI-dependent necroptosis by the Z-DNA binding domain of the vaccinia virus innate immune evasion protein, E3,” *Proceedings of the National Academy of Sciences*, vol. 114, no. 43, pp. 11506–11511, 2017.

[20] W. D. Arndt *et al.*, “Evasion of the Innate Immune Type I Interferon System by Monkeypox Virus,” *Journal of Virology*, vol. 89, no. 20, pp. 10489–10499, Oct. 2015, doi: 10.1128/JVI.00304-15.

[21] J. O. Langland and B. L. Jacobs, “Inhibition of PKR by vaccinia virus: role of the N-and C-terminal domains of E3L,” *Virology*, vol. 324, no. 2, pp. 419–429, 2004.

[22] R. Buller and G. J. Palumbo, “Poxvirus pathogenesis,” *Microbiological reviews*, vol. 55, no. 1, pp. 80–122, 1991.

[23] A. Peisley and S. Hur, “Multi-level regulation of cellular recognition of viral dsRNA,” *Cell. Mol. Life Sci.*, vol. 70, no. 11, pp. 1949–1963, Jun. 2013, doi: 10.1007/s00018-012-1149-4.

[24] X. Sun, J. Yin, M. A. Starovasnik, W. J. Fairbrother, and V. M. Dixit, “Identification of a Novel Homotypic Interaction Motif Required for the Phosphorylation of Receptor-interacting Protein (RIP) by RIP3 *,” *Journal of Biological Chemistry*, vol. 277, no. 11, pp. 9505–9511, Mar. 2002, doi: 10.1074/jbc.M109488200.

[25] X. Sun, J. Lee, T. Navas, D. T. Baldwin, T. A. Stewart, and V. M. Dixit, “RIP3, a novel apoptosis-inducing kinase,” *Journal of Biological Chemistry*, vol. 274, no. 24, pp. 16871–16875, 1999.

[26] W. J. Kaiser *et al.*, “Toll-like Receptor 3-mediated Necrosis via TRIF, RIP3, and MLKL,” *J Biol Chem*, vol. 288, no. 43, pp. 31268–31279, Oct. 2013, doi: 10.1074/jbc.M113.462341.

[27] J. W. Upton, W. J. Kaiser, and E. S. Mocarski, “DAI/ZBP1/DLM-1 Complexes with RIP3 to Mediate Virus-Induced Programmed Necrosis that Is Targeted by Murine Cytomegalovirus vIRA,” *Cell Host & Microbe*, vol. 11, no. 3, pp. 290–297, Mar. 2012, doi: 10.1016/j.chom.2012.01.016.

[28] Y. Dondelinger *et al.*, “MLKL compromises plasma membrane integrity by binding to phosphatidylinositol phosphates,” *Cell reports*, vol. 7, no. 4, pp. 971–981, 2014.

[29] H. Wang *et al.*, “Mixed Lineage Kinase Domain-like Protein MLKL Causes Necrotic Membrane Disruption upon Phosphorylation by RIP3,” *Molecular Cell*, vol. 54, no. 1, pp. 133–146, Apr. 2014, doi: 10.1016/j.molcel.2014.03.003.

[30] R. J. Thapa *et al.*, “Interferon-induced RIP1/RIP3-mediated necrosis requires PKR and is licensed by FADD and caspases,” *Proceedings of the National Academy of Sciences*, vol. 110, no. 33, pp. E3109–E3118, Aug. 2013, doi: 10.1073/pnas.1301218110.

[31] S. McComb *et al.*, “Type-I interferon signaling through ISGF3 complex is required for sustained Rip3 activation and necroptosis in macrophages,” *Proceedings of the National Academy of Sciences*, vol. 111, no. 31, pp. E3206–E3213, Aug. 2014, doi: 10.1073/pnas.1407068111.

[32] D. Yang *et al.*, "ZBP1 mediates interferon-induced necroptosis," *Cell Mol Immunol*, vol. 17, no. 4, Art. no. 4, Apr. 2020, doi: 10.1038/s41423-019-0237-x.

[33] Z. Liu *et al.*, "A class of viral inducer of degradation of the necroptosis adaptor RIPK3 regulates virus-induced inflammation," *Immunity*, vol. 54, no. 2, pp. 247-258.e7, Feb. 2021, doi: 10.1016/j.immuni.2020.11.020.

[34] A. Hershko and A. Ciechanover, "THE UBIQUITIN SYSTEM," p. 57, 1998.

[35] D. Skowyra, K. L. Craig, M. Tyers, S. J. Elledge, and J. W. Harper, "F-Box Proteins Are Receptors that Recruit Phosphorylated Substrates to the SCF Ubiquitin-Ligase Complex," *Cell*, vol. 91, no. 2, pp. 209–219, Oct. 1997, doi: 10.1016/S0092-8674(00)80403-1.

[36] H. Koehler *et al.*, "Vaccinia virus E3 prevents sensing of Z-RNA to block ZBP1-dependent necroptosis," *Cell Host & Microbe*, vol. 29, no. 8, pp. 1266-1276.e5, Aug. 2021, doi: 10.1016/j.chom.2021.05.009.

[37] W. D. Arndt *et al.*, "Monkeypox virus induces the synthesis of less dsRNA than vaccinia virus, and is more resistant to the anti-poxvirus drug, IBT, than vaccinia virus," *Virology*, vol. 497, pp. 125–135, 2016.

[38] S. G. Cresawn and R. C. Condit, "A targeted approach to identification of vaccinia virus postreplicative transcription elongation factors: Genetic evidence for a role of the H5R gene in vaccinia transcription," *Virology*, vol. 363, no. 2, pp. 333–341, Jul. 2007, doi: 10.1016/j.virol.2007.02.016.

[39] S. Nogusa *et al.*, "RIPK3 Activates Parallel Pathways of MLKL-Driven Necroptosis and FADD-Mediated Apoptosis to Protect against Influenza A Virus," *Cell Host & Microbe*, vol. 20, no. 1, pp. 13–24, Jul. 2016, doi: 10.1016/j.chom.2016.05.011.

[40] B. P. Daniels *et al.*, "The Nucleotide Sensor ZBP1 and Kinase RIPK3 Induce the Enzyme IRG1 to Promote an Antiviral Metabolic State in Neurons," *Immunity*, vol. 50, no. 1, pp. 64-76.e4, Jan. 2019, doi: 10.1016/j.immuni.2018.11.017.

[41] S. G. Cresawn, C. Prins, D. R. Latner, and R. C. Condit, "Mapping and phenotypic analysis of spontaneous isatin-β-thiosemicarbazone resistant mutants of vaccinia virus," *Virology*, vol. 363, no. 2, pp. 319–332, 2007.

[42] T. Shors, K. V. Kibler, K. B. Perkins, R. Seidler-Wulff, M. P. Banaszak, and B. L. Jacobs, "Complementation of Vaccinia Virus Deleted of the E3L Gene by Mutants of E3L," *Virology*, vol. 239, no. 2, pp. 269–276, Dec. 1997, doi: 10.1006/viro.1997.8881.

CHAPTER 4

DISCUSSION AND FUTURE DIRECTIONS

Type I IFNs are an important first defense against pathogens in mediating the activation of innate and adaptive immune responses. VACV has been shown to inhibit the host's antiviral immune response by inhibiting the IFN response through the E3 protein [84]. The E3 protein is comprised of two conserved domains: the N-terminal Z-nucleic acid binding domain (Z-BD) and the C-terminal double-stranded RNA-binding domain (dsRBD). The dsRBD has been shown to bind dsRNA and sequester it away from known PRRs, such as PKR and OAS. The function of the N-terminal Z-BD has been more elusive. The N-terminus of E3 has been shown to be required for pathogenesis and for IFN resistance in 129 MEFs and L929 cells, and for replication in JC cells [81], [89 – 91]. It is also required to fully inhibit PKR in 129 MEFs, HeLa cells, and in the mouse model [91 – 92]. The N-terminus of E3 is also necessary to inhibit IFN-primed necroptosis in a ZBP1- and RIPK3- dependent manner, as VACV E3 mutants that were missing the Z-BD died rapidly [81], [93]. The E3 homologue in MPXV, F3, has a natural truncation at the N-terminus due to the loss of the first 37 amino acids. This makes the F3 resemble the E3 protein of VACV-E3LΔ37N, which is also missing 37 amino acids from the N-terminus. However, VACV-E3LΔ37N pathogenesis is attenuated in the mice model and leads to activation of the PKR pathway, while MPXV retains pathogenesis and evades PKR recognition [90]. In addition, VACV-E3LΔ37N does not replicate in JC cells while MPXV replicates to VACV WT levels.

In this study, we started by investigating whether MPXV was resistant to type I IFN and if it induced necroptosis. In chapter 2 we show that IFNα inhibits MPXV

replication in L929 cells and 10 U of IFN is able to reduce MPXV plaque formation by 50%. We determined that this IFN sensitivity was fully dependent on ZBP1, RIPK3, MLKL, but not PKR. ZBP1 has been shown to initiate necroptosis through binding of Z-DNA/RNA which activates RIPK3 through RHIM-RHIM interaction and leads to cell death through MLKL phosphorylation and trimerization [69]. We deleted ZBP1, RIPK3, and MLKL from L929 cells with the CRISPR/Cas9 system and were able to rescue MPXV and VACV-E3LΔ37N viral replication and IFN resistance.

It was surprising that the IFN sensitivity of MPXV was dependent on the necroptotic proteins, since MPXV does not seem to induce necroptosis in L929 cells, even with the addition of a pancaspase inhibitor, we failed to see trimerized MLKL or loss of membrane integrity. We hypothesized that the reason why MPXV was not inducing necroptosis was because RIPK3 was being degraded by the viral inducer of RIPK3 degradation (vIRD), as was reported for CPXV [94]. We observed that RIPK3 was indeed being degraded in CPXV and MPXV infected cells, but not in VACV or VACV-E3LΔ37N infected cells as VACV vIRD is truncated and missing the C-terminal F-Box [94]. RIPK3 protein levels in MPXV infected cells were not completely degraded when compared to CPXV samples and this could be due to a timing issue of harvesting the samples before RIPK3 was completely degraded, or RIPK3 could be signaling or forming an unknown complex that would render it inaccessible. Next, we inhibited RIPK3 cleavage by MPXV and CPXV using a pancaspase inhibitor, zVAD-FMK. The mechanism for RIPK3 degradation inhibition by zVAD-FMK is unclear, as we expected zVAD-FMK to inhibit apoptosis, leaving MPXV vIRD to cleave RIPK3. The Skp1-Cullin1-F-box (SCF) Cullin-Ring containing Skp2 has been shown to interact with

TRAIL-R2 and the death-inducing signaling complex (DISC) through the cellular FLICE-like inhibitory protein (FLIP (L)), where procaspase-8 is also recruited [95]. Perhaps caspases are also required for RIPK3 recruitment to the SCF complex, and addition of zVAD-FMK could have prevented this from occurring.

VACV contains many proteins to inhibit apoptosis and necroptosis, such as B13 (SPI-2), B22 (SPI-1), F1, N1, and the E3 protein. As we've shown here, and by Koehler et al. [81], [93], the N-terminus of the E3 protein is essential for inhibiting ZPB1-dependent necroptosis. MPXV seems to not inhibit apoptosis as well as VACV, as it was demonstrated that it induces apoptosis in cells [96]. The less pathogenic strain of MPXV, Clade 2b, also lacks the full-length BR-203 virulence factor that inhibits apoptosis, suggesting that MPXV has evolved mechanisms to avoid necroptosis through apoptosis as a means to counteract loss of a functional N-terminus.

Both zVAD-FMK and the neddylation inhibitor, MLN4924, restored RIPK3 protein expression, but only in CPXV infected cells did we observe necroptosis as detected by trimerization of MLKL and plasma membrane integrity. MPXV infected cells did not induce necroptosis, despite having RIPK3 present, signifying that MPXV has an additional way to inhibit necroptosis through a yet unknown mechanism. Cell death, whether apoptosis or necroptosis, is the last option for the host to control a viral infection. When a cell dies, the virus can no longer use the host machinery for replication, and this places a limit on viral spread. Thus, viruses have evolved different mechanisms to block different steps in these death pathways, placing pressure on the host to evolve due to these virus-encoded death suppressors. DNA viruses, such as VACV and cytomegalovirus (CMV) have developed ways to not only inhibit apoptosis through

caspase 8 inhibition, but can also inhibit necroptosis. Herpes simplex virus (HSV)-1 and HSV-2 are significant human pathogens that block apoptosis through binding to and blocking caspase 8 using the large subunit (R1) of the ribonucleotide reductase (RR). It has also been shown that HSV-1 and HSV-2 can block necroptosis through the RHIM containing R1 proteins (ICP6 and ICP10) and inhibit the interaction between RIPK1 and RIPK3 [14]. Interestingly, some poxvirus genomes contain sequence similarities to MLKL and expression of these genes leads to inhibition of MLKL and cell death [17]. Additionally, the human CMV major immediate early 1 (IE3) protein has been shown to suppress necroptosis post RIPK3 phosphorylation by an unknown mechanism [18]. Thus, it is of no surprise that MPXV has evolved mechanisms in necroptosis inhibition. It would be interesting to insert MPXV vIRD into low dsRNA producing VACV-E3LΔ37N and this would confirm that the first step in necroptosis inhibition in MPXV infection is due to RIPK3 degradation.

We examined the last step in necroptosis involving MLKL to determine the location of inhibition. We were able to separate phosphorylated MLKL into cytoplasmic and membrane bound fractions to visualize the inhibition step in MPXV infected cells. In MPXV infection, MLKL gets phosphorylated on Ser358 only with the addition of zVAD or MLN4924 and travels to the plasma membrane, but it does not trimerize. TAM (Tyro3, Axl, and Mer) kinases have been shown to be promoters of necroptosis by phosphorylating MLKL on a second site at Tyr376, a step required for MLKL trimerization [72]. We've seen that Tyro376 gets phosphorylated only in VACV-E3LΔ37N infection [97], but not with MPXV (data not shown). Suggesting that MPXV

is inhibiting necroptosis by blocking the phosphorylation of Tyr376 by TAM kinases. Future experiments will need to examine if and how this inhibition is occurring.

Even though the E3 homologue in MPXV is truncated, MPXV has evolved ways to maintain its pathogenicity and one of the ways it does this is through inhibition of the necroptosis pathway. In this study, we show that L929 cells inhibit MPXV viral replication through the type I IFN pathway that is ZBP1-, RIPK3-, and MLKL-dependent. MPXV has evolved two ways to inhibit necroptosis. It degrades RIPK3 and prevents necrosome formation and it also prevents MLKL from trimerizing at the plasma membrane. We also show the potential for new anti-MPXV treatment using an IFN inducer, either with a pancaspase inhibitor or a proteasome inhibitor, as they limit MPXV replication without the potential inflammatory effects of necroptosis. However, the anti-MPXV effects of these drugs will have to be assessed in the mice model first.

MPXV makes less dsRNA than VACV or VACV- E3LΔ37N and evades PKR and is able to replicate to VACV WT levels [98]. Like we showed in chapter 2 with L929 cells, MPXV also does not induce necroptosis in JC cells, however the mechanisms for inhibition are different. The MPXV vIRD in JC cells completely cleaves RIPK3 and we were able to induce necroptosis in MPXV infected cells by inhibiting RIPK3 degradation with a neddylation inhibitor. In L929 cells infected with VACV N-terminal deletion mutants, necroptosis is the main form of anti-viral regulation dependent on ZBP1 and RIPK3 through sensing of Z-RNA. In JC cells, we demonstrate that PKR plays a role in viral-induced necroptosis.

Necroptosis can be initiated through TLR3, TLR4, TNFR, or ZBP1. Data from the Balachandran lab implicated PKR in necroptosis in 2013 and to our knowledge, no

other study has been published since then. They showed that when FADD or caspases are inhibited, IFN activates PKR which then activates the RIPK1/RIPK3 necroptotic pathway. PKR has never before been shown to be important for pathogen-induced necroptosis. In chapter 3 we demonstrate that cell viability in JC cells can be recovered by reducing the amount of dsRNA formed during virus infection and by deleting PKR. However, reducing the amount of dsRNA produced using VACV- E3LΔ37N IBTR3 and VACV- E3LΔ37N IBTR7 viruses was not sufficient to recover viral growth. Suggesting that a second pathway is involved in viral inhibition. When the RIPK3 inhibitor was added to the low dsRNA producing VACV mutants, viral replication was rescued, signifying that RIPK3 is a crucial component of viral regulation as CRISPR KO of RIPK3 also restored viral replication. In addition to necroptosis, RIPK3 can activate apoptosis in a FADD-dependent manner during influenza A virus (IAV) infection [99]. Daniels et al. also showed that ZBP1 senses Zika virus (ZIKV) infection in neurons and leads to RIPK3 activation, however the inhibition of viral replication is not due to necroptosis. RIPK3 leads to the production of the metabolite Itaconate that induces an antiviral state that inhibits viral replication [100]. The mechanism of viral regulation by RIPK3 and what is activating it is unclear. Crosslinking experiments and/or CO-IPs will be essential in showing what RIPK3 is bound to and what other proteins are in the necrosome. We hypothesize that there are at least two or more pathways controlling poxviral replication. The first is that PKR is binding to RIPK1/RIPK3, as Thapa et al. showed that PKR can physically associate with RIPK1 *in vitro*, suggesting that it can directly phosphorylate RIPK1. The second is that RIPK3 is activating a non-necroptotic pathway that could be activated if PKR or ZBP1 are inhibited.

Overall, in this study we investigated the ability of MPXV to inhibit necroptosis in two cell lines, L929 and JC cells, and ways the cells combat MPXV and VACV infections. We found that IFN treatment efficiently inhibits MPXV replication, and we found new link between PKR and viral-induced necroptosis. We hope that our data can translate *in vivo* and aid in combating the current MPXV outbreak by helping in the development of additional anti-orthopoxvirus drugs.

REFERENCES

[1] P. von Magnus, E. K. Andersen, K. B. Petersen, and A. Birch-Andersen, “A pox-like disease in cynomolgus monkeys,” *Acta Pathologica Microbiologica Scandinavica*, vol. 46, no. 2, pp. 156–176, 1959.

[2] I. D. Ladnyj, P. Ziegler, and E. Kima, “A human infection caused by monkeypox virus in Basankusu Territory, Democratic Republic of the Congo,” *Bull World Health Organ*, vol. 46, no. 5, pp. 593–597, 1972.

[3] S. Parker, A. Nuara, R. M. L. Buller, and D. A. Schultz, “Human monkeypox: an emerging zoonotic disease,” 2007.

[4] J. G. Breman, M. Kalisa-Ruti, E. Zanotto, A. Gromyko, and I. Arita, “Human monkeypox, 1970-79,” *Bulletin of the World Health Organization*, vol. 58, no. 2, p. 165, 1980.

[5] K. D. Reed *et al.*, “The detection of monkeypox in humans in the Western Hemisphere,” *New England Journal of Medicine*, vol. 350, no. 4, pp. 342–350, 2004.

[6] A. M. Likos *et al.*, “A tale of two clades: monkeypox viruses,” *Journal of General Virology*, vol. 86, no. 10, pp. 2661–2672, doi: 10.1099/vir.0.81215-0.

[7] J. R. Weaver and S. N. Isaacs, “Monkeypox virus and insights into its immunomodulatory proteins,” *Immunological Reviews*, vol. 225, no. 1, pp. 96–113, 2008, doi: 10.1111/j.1600-065X.2008.00691.x.

[8] N. Chen *et al.*, “Virulence differences between monkeypox virus isolates from West Africa and the Congo basin,” *Virology*, vol. 340, no. 1, pp. 46–63, Sep. 2005, doi: 10.1016/j.virol.2005.05.030.

[9] N. Kumar, A. Acharya, H. E. Gendelman, and S. N. Byrareddy, “The 2022 outbreak and the pathobiology of the monkeypox virus,” *Journal of Autoimmunity*, vol. 131, p. 102855, Jul. 2022, doi: 10.1016/j.jaut.2022.102855.

[10] Q. Gong, C. Wang, X. Chuai, and S. Chiu, “Monkeypox virus: a re-emergent threat to humans,” *Virologica Sinica*, vol. 37, no. 4, pp. 477–482, Aug. 2022, doi: 10.1016/j.virs.2022.07.006.

[11] J. G. Rizk, G. Lippi, B. M. Henry, D. N. Forthal, and Y. Rizk, “Prevention and Treatment of Monkeypox,” *Drugs*, vol. 82, no. 9, pp. 957–963, Jun. 2022, doi: 10.1007/s40265-022-01742-y.

[12] A. C. Townsley, A. S. Weisberg, T. R. Wagenaar, and B. Moss, “Vaccinia virus entry into cells via a low-pH-dependent endosomal pathway,” *Journal of virology*, vol. 80, no. 18, pp. 8899–8908, 2006.

[13] J.-C. Hsiao, C.-S. Chung, and W. Chang, “Vaccinia Virus Envelope D8L Protein Binds to Cell Surface Chondroitin Sulfate and Mediates the Adsorption of Intracellular Mature Virions to Cells,” *Journal of Virology*, vol. 73, no. 10, pp. 8750–8761, Oct. 1999, doi: 10.1128/JVI.73.10.8750-8761.1999.

[14] C.-S. Chung, J.-C. Hsiao, Y.-S. Chang, and W. Chang, “A27L Protein Mediates Vaccinia Virus Interaction with Cell Surface Heparan Sulfate,” *Journal of Virology*, vol. 72, no. 2, pp. 1577–1585, Feb. 1998, doi: 10.1128/JVI.72.2.1577-1585.1998.

[15] C.-L. Lin, C.-S. Chung, H. G. Heine, and W. Chang, “Vaccinia Virus Envelope H3L Protein Binds to Cell Surface Heparan Sulfate and Is Important for Intracellular Mature Virion Morphogenesis and Virus Infection In Vitro and In Vivo,” *Journal of Virology*, vol. 74, no. 7, pp. 3353–3365, Apr. 2000, doi: 10.1128/JVI.74.7.3353-3365.2000.

[16] M.-I. Vázquez and M. Esteban, “Identification of Functional Domains in the 14-Kilodalton Envelope Protein (A27L) of Vaccinia Virus,” *Journal of Virology*, vol. 73, no. 11, pp. 9098–9109, Nov. 1999, doi: 10.1128/JVI.73.11.9098-9109.1999.

[17] W.-L. Chiu, C.-L. Lin, M.-H. Yang, D.-L. M. Tzou, and W. Chang, “Vaccinia Virus 4c (A26L) Protein on Intracellular Mature Virus Binds to the Extracellular Cellular Matrix Laminin,” *Journal of Virology*, vol. 81, no. 5, pp. 2149–2157, Mar. 2007, doi: 10.1128/JVI.02302-06.

[18] T. G. Senkevich, S. Ojeda, A. Townsley, G. E. Nelson, and B. Moss, “Poxvirus multiprotein entry–fusion complex,” *Proceedings of the National Academy of Sciences*, vol. 102, no. 51, pp. 18572–18577, 2005.

[19] B. Moss, “Poxvirus cell entry: how many proteins does it take?,” *Viruses*, vol. 4, no. 5, pp. 688–707, 2012.

[20] G. McFadden, “Poxvirus tropism,” *Nat Rev Microbiol*, vol. 3, no. 3, Art. no. 3, Mar. 2005, doi: 10.1038/nrmicro1099.

[21] S. S. Y. 2003 Broyles, “Vaccinia virus transcription,” *Journal of General Virology*, vol. 84, no. 9, pp. 2293–2303, doi: 10.1099/vir.0.18942-0.

[22] Z. Yang, S. E. Reynolds, C. A. Martens, D. P. Bruno, S. F. Porcella, and B. Moss, “Expression Profiling of the Intermediate and Late Stages of Poxvirus Replication,” *Journal of Virology*, vol. 85, no. 19, pp. 9899–9908, Oct. 2011, doi: 10.1128/JVI.05446-11.

[23] B. M. Baroudy, S. Venkatesan, and B. Moss, “Structure and Replication of Vaccinia Virus Telomeres,” *Cold Spring Harb Symp Quant Biol*, vol. 47, pp. 723–729, Jan. 1983, doi: 10.1101/SQB.1983.047.01.083.

[24] P. Geshelin and K. I. Berns, “Characterization and localization of the naturally occurring cross-links in vaccinia virus DNA,” *Journal of Molecular Biology*, vol. 88, no. 4, pp. 785–796, Oct. 1974, doi: 10.1016/0022-2836(74)90399-4.

[25] M. W. Czarnecki and P. Traktman, “The vaccinia virus DNA polymerase and its processivity factor,” *Virus research*, vol. 234, pp. 193–206, 2017.

[26] S. C. Rochester and P. Traktman, “Characterization of the single-stranded DNA binding protein encoded by the vaccinia virus I3 gene,” *Journal of virology*, vol. 72, no. 4, pp. 2917–2926, 1998.

[27] S. Welsch, L. Doglio, S. Schleich, and J. Krijnse Locker, “The Vaccinia Virus I3L Gene Product Is Localized to a Complex Endoplasmic Reticulum-Associated Structure That Contains the Viral Parental DNA,” *Journal of Virology*, vol. 77, no. 10, pp. 6014–6028, May 2003, doi: 10.1128/JVI.77.10.6014-6028.2003.

[28] C. Colby and P. Duesberg, “Double-stranded RNA in vaccinia virus infected cells,” *Nature*, vol. 222, no. 5197, pp. 940–944, 1969.

[29] P. Duesberg and C. Colby, “On the biosynthesis and structure of double-stranded RNA in vaccinia virus-infected cells,” *Proceedings of the National Academy of Sciences*, vol. 64, no. 1, pp. 396–403, 1969.

[30] R. C. Condit, N. Moussatche, and P. Traktman, “In A Nutshell: Structure and Assembly of the Vaccinia Virion,” in *Advances in Virus Research*, vol. 66, Academic Press, 2006, pp. 31–124. doi: 10.1016/S0065-3527(06)66002-8.

[31] C. Morgan, “The Insertion of DNA into Vaccinia Virus,” *Science*, vol. 193, no. 4253, pp. 591–592, Aug. 1976, doi: 10.1126/science.959819.

[32] S. Dales and E. H. Mosbach, “Vaccinia as a model for membrane biogenesis,” *Virology*, vol. 35, no. 4, pp. 564–583, 1968.

[33] M. Schmelz *et al.*, “Assembly of vaccinia virus: the second wrapping cisterna is derived from the trans Golgi network,” *Journal of Virology*, vol. 68, no. 1, pp. 130–147, Jan. 1994, doi: 10.1128/jvi.68.1.130-147.1994.

[34] G. Sivan, A. S. Weisberg, J. L. Americo, and B. Moss, “Retrograde Transport from Early Endosomes to the trans-Golgi Network Enables Membrane Wrapping and

Egress of Vaccinia Virus Virions," *Journal of Virology*, vol. 90, no. 19, pp. 8891–8905, Sep. 2016, doi: 10.1128/JVI.01114-16.

[35] J. Wu *et al.*, "Cyclic GMP-AMP Is an Endogenous Second Messenger in Innate Immune Signaling by Cytosolic DNA," *Science*, vol. 339, no. 6121, pp. 826–830, Feb. 2013, doi: 10.1126/science.1229963.

[36] L. Sun, J. Wu, F. Du, X. Chen, and Z. J. Chen, "Cyclic GMP-AMP Synthase Is a Cytosolic DNA Sensor That Activates the Type I Interferon Pathway," *Science*, vol. 339, no. 6121, pp. 786–791, Feb. 2013, doi: 10.1126/science.1232458.

[37] M. Yoneyama *et al.*, "The RNA helicase RIG-I has an essential function in double-stranded RNA-induced innate antiviral responses," *Nat Immunol*, vol. 5, no. 7, Art. no. 7, Jul. 2004, doi: 10.1038/ni1087.

[38] L. Alexopoulou, A. C. Holt, R. Medzhitov, and R. A. Flavell, "Recognition of double-stranded RNA and activation of NF-κB by Toll-like receptor 3," *Nature*, vol. 413, no. 6857, Art. no. 6857, Oct. 2001, doi: 10.1038/35099560.

[39] M. Brisse and H. Ly, "Comparative Structure and Function Analysis of the RIG-I-Like Receptors: RIG-I and MDA5," *Frontiers in Immunology*, vol. 10, 2019, Accessed: Aug. 25, 2022. [Online]. Available: https://www.frontiersin.org/articles/10.3389/fimmu.2019.01586

[40] V. Hornung *et al.*, "5'-Triphosphate RNA Is the Ligand for RIG-I," *Science*, vol. 314, no. 5801, pp. 994–997, Nov. 2006, doi: 10.1126/science.1132505.

[41] S. Myong *et al.*, "Cytosolic Viral Sensor RIG-I Is a 5'-Triphosphate–Dependent Translocase on Double-Stranded RNA," *Science*, vol. 323, no. 5917, pp. 1070–1074, Feb. 2009, doi: 10.1126/science.1168352.

[42] H. Kato *et al.*, "Length-dependent recognition of double-stranded ribonucleic acids by retinoic acid–inducible gene-I and melanoma differentiation–associated gene 5," *Journal of Experimental Medicine*, vol. 205, no. 7, pp. 1601–1610, Jun. 2008, doi: 10.1084/jem.20080091.

[43] J. Rehwinkel and M. U. Gack, "RIG-I-like receptors: their regulation and roles in RNA sensing," *Nat Rev Immunol*, vol. 20, no. 9, Art. no. 9, Sep. 2020, doi: 10.1038/s41577-020-0288-3.

[44] R. B. Seth, L. Sun, C.-K. Ea, and Z. J. Chen, "Identification and Characterization of MAVS, a Mitochondrial Antiviral Signaling Protein that Activates NF-κB and IRF3," *Cell*, vol. 122, no. 5, pp. 669–682, Sep. 2005, doi: 10.1016/j.cell.2005.08.012.

[45] M. Yamamoto *et al.*, “Role of Adaptor TRIF in the MyD88-Independent Toll-Like Receptor Signaling Pathway,” *Science*, vol. 301, no. 5633, pp. 640–643, Aug. 2003, doi: 10.1126/science.1087262.

[46] L. Liu *et al.*, “Structural Basis of Toll-Like Receptor 3 Signaling with Double-Stranded RNA,” *Science*, vol. 320, no. 5874, pp. 379–381, Apr. 2008, doi: 10.1126/science.1155406.

[47] T. Kawasaki and T. Kawai, “Toll-Like Receptor Signaling Pathways,” *Frontiers in Immunology*, vol. 5, 2014, Accessed: Aug. 28, 2022. [Online]. Available: https://www.frontiersin.org/articles/10.3389/fimmu.2014.00461

[48] L. B. Ivashkiv and L. T. Donlin, “Regulation of type I interferon responses,” *Nat Rev Immunol*, vol. 14, no. 1, Art. no. 1, Jan. 2014, doi: 10.1038/nri3581.

[49] “The JAK-STAT Pathway at Twenty,” *Immunity*, vol. 36, no. 4, pp. 503–514, Apr. 2012, doi: 10.1016/j.immuni.2012.03.013.

[50] F. McNab, K. Mayer-Barber, A. Sher, A. Wack, and A. O’Garra, “Type I interferons in infectious disease,” *Nat Rev Immunol*, vol. 15, no. 2, Art. no. 2, Feb. 2015, doi: 10.1038/nri3787.

[51] A. Wack, E. Terczyńska-Dyla, and R. Hartmann, “Guarding the frontiers: the biology of type III interferons,” *Nat Immunol*, vol. 16, no. 8, Art. no. 8, Aug. 2015, doi: 10.1038/ni.3212.

[52] W. K. Roberts, A. Hovanessian, R. E. Brown, M. J. Clemens, and I. M. Kerr, “Interferon-mediated protein kinase and low-molecular-weight inhibitor of protein synthesis,” *Nature*, vol. 264, no. 5585, Art. no. 5585, Dec. 1976, doi: 10.1038/264477a0.

[53] B. Lebleu, G. C. Sen, S. Shaila, B. Cabrer, and P. Lengyel, “Interferon, double-stranded RNA, and protein phosphorylation.,” *Proceedings of the National Academy of Sciences*, vol. 73, no. 9, pp. 3107–3111, Sep. 1976, doi: 10.1073/pnas.73.9.3107.

[54] A. G. Hovanessian, “On the discovery of interferon-inducible, double-stranded RNA activated enzymes: The 2′–5′oligoadenylate synthetases and the protein kinase PKR,” *Cytokine & Growth Factor Reviews*, vol. 18, no. 5, pp. 351–361, Oct. 2007, doi: 10.1016/j.cytogfr.2007.06.003.

[55] J. Galabru and A. Hovanessian, “Autophosphorylation of the protein kinase dependent on double-stranded RNA.,” *Journal of Biological Chemistry*, vol. 262, no. 32, pp. 15538–15544, Nov. 1987, doi: 10.1016/S0021-9258(18)47759-9.

[56] R. E. Rhoads, “Regulation of eukaryotic protein synthesis by initiation factors.,” *Journal of Biological Chemistry*, vol. 268, no. 5, pp. 3017–3020, 1993.

[57] H. Yu, R. C. Bruneau, G. Brennan, and S. Rothenburg, “Battle Royale: Innate Recognition of Poxviruses and Viral Immune Evasion,” *Biomedicines*, vol. 9, no. 7, Art. no. 7, Jul. 2021, doi: 10.3390/biomedicines9070765.

[58] R. H. Silverman, “Viral Encounters with 2′,5′-Oligoadenylate Synthetase and RNase L during the Interferon Antiviral Response,” *Journal of Virology*, vol. 81, no. 23, pp. 12720–12729, Dec. 2007, doi: 10.1128/JVI.01471-07.

[59] T. Schwartz, J. Behlke, K. Lowenhaupt, U. Heinemann, and A. Rich, “Structure of the DLM-1–Z-DNA complex reveals a conserved family of Z-DNA-binding proteins,” *Nat Struct Mol Biol*, vol. 8, no. 9, Art. no. 9, Sep. 2001, doi: 10.1038/nsb0901-761.

[60] A. Rich and S. Zhang, “Z-DNA: the long road to biological function,” *Nature Reviews Genetics*, vol. 4, no. 7, pp. 566–572, 2003.

[61] A. H.-J. Wang *et al.*, “Molecular structure of a left-handed double helical DNA fragment at atomic resolution,” *Nature*, vol. 282, no. 5740, pp. 680–686, 1979.

[62] B. Wittig, T. Dorbic, and A. Rich, “The level of Z-DNA in metabolically active, permeabilized mammalian cell nuclei is regulated by torsional strain.,” *Journal of Cell Biology*, vol. 108, no. 3, pp. 755–764, Mar. 1989, doi: 10.1083/jcb.108.3.755.

[63] G. P. Schroth, P.-J. Chou, and P. S. Ho, “Mapping Z-DNA in the human genome. Computer-aided mapping reveals a nonrandom distribution of potential Z-DNA-forming sequences in human genes.,” *Journal of Biological Chemistry*, vol. 267, no. 17, pp. 11846–11855, 1992.

[64] L. F. Liu and J. C. Wang, “Supercoiling of the DNA template during transcription.,” *Proceedings of the National Academy of Sciences*, vol. 84, no. 20, pp. 7024–7027, Oct. 1987, doi: 10.1073/pnas.84.20.7024.

[65] S. C. Ha, D. Kim, H.-Y. Hwang, A. Rich, Y.-G. Kim, and K. K. Kim, “The crystal structure of the second Z-DNA binding domain of human DAI (ZBP1) in complex with Z-DNA reveals an unusual binding mode to Z-DNA,” *PNAS*, vol. 105, no. 52, pp. 20671–20676, Dec. 2008, doi: 10.1073/pnas.0810463106.

[66] W. J. Kaiser, J. W. Upton, and E. S. Mocarski, “Receptor-Interacting Protein Homotypic Interaction Motif-Dependent Control of NF-κB Activation via the DNA-Dependent Activator of IFN Regulatory Factors,” *The Journal of Immunology*, vol. 181, no. 9, pp. 6427–6434, Nov. 2008, doi: 10.4049/jimmunol.181.9.6427.

[67] M. Li and A. A. Beg, “Induction of Necrotic-Like Cell Death by Tumor Necrosis Factor Alpha and Caspase Inhibitors: Novel Mechanism for Killing Virus-Infected Cells,” *Journal of Virology*, vol. 74, no. 16, pp. 7470–7477, Aug. 2000, doi: 10.1128/JVI.74.16.7470-7477.2000.

[68] O. Micheau and J. Tschopp, “Induction of TNF Receptor I-Mediated Apoptosis via Two Sequential Signaling Complexes,” *Cell*, vol. 114, no. 2, pp. 181–190, Jul. 2003, doi: 10.1016/S0092-8674(03)00521-X.

[69] Y. K. Dhuriya and D. Sharma, “Necroptosis: a regulated inflammatory mode of cell death,” *Journal of Neuroinflammation*, vol. 15, no. 1, p. 199, Jul. 2018, doi: 10.1186/s12974-018-1235-0.

[70] M. A. O’Donnell *et al.*, “Caspase 8 inhibits programmed necrosis by processing CYLD,” *Nature cell biology*, vol. 13, no. 12, pp. 1437–1442, 2011.

[71] Y. Dondelinger *et al.*, “MLKL compromises plasma membrane integrity by binding to phosphatidylinositol phosphates,” *Cell reports*, vol. 7, no. 4, pp. 971–981, 2014.

[72] A. Najafov *et al.*, “TAM Kinases Promote Necroptosis by Regulating Oligomerization of MLKL,” *Molecular Cell*, vol. 75, no. 3, pp. 457-468.e4, Aug. 2019, doi: 10.1016/j.molcel.2019.05.022.

[73] J. M. Murphy *et al.*, “The pseudokinase MLKL mediates necroptosis via a molecular switch mechanism,” *Immunity*, vol. 39, no. 3, pp. 443–453, 2013.

[74] C. Zhan, M. Huang, X. Yang, and J. Hou, “MLKL: Functions beyond serving as the Executioner of Necroptosis,” *Theranostics*, vol. 11, no. 10, pp. 4759–4769, Mar. 2021, doi: 10.7150/thno.54072.

[75] Z. Cai *et al.*, “Plasma membrane translocation of trimerized MLKL protein is required for TNF-induced necroptosis,” *Nature Cell Biology*, vol. 16, no. 1, pp. 55–65, Jan. 2014, doi: 10.1038/ncb2883.

[76] S. He, Y. Liang, F. Shao, and X. Wang, “Toll-like receptors activate programmed necrosis in macrophages through a receptor-interacting kinase-3—mediated pathway,” *Proceedings of the National Academy of Sciences of the United States of America*, vol. 108, no. 50, pp. 20054–20059, 2011.

[77] W. J. Kaiser *et al.*, “Toll-like Receptor 3-mediated Necrosis via TRIF, RIP3, and MLKL,” *J Biol Chem*, vol. 288, no. 43, pp. 31268–31279, Oct. 2013, doi: 10.1074/jbc.M113.462341.

[78] J. W. Upton, W. J. Kaiser, and E. S. Mocarski, “Cytomegalovirus M45 cell death suppression requires receptor-interacting protein (RIP) homotypic interaction motif

(RHIM)-dependent interaction with RIP1," *J. Biol. Chem.*, vol. 283, no. 25, pp. 16966–16970, Jun. 2008, doi: 10.1074/jbc.C800051200.

[79] J. W. Upton, W. J. Kaiser, and E. S. Mocarski, "DAI/ZBP1/DLM-1 Complexes with RIP3 to Mediate Virus-Induced Programmed Necrosis that Is Targeted by Murine Cytomegalovirus vIRA," *Cell Host & Microbe*, vol. 11, no. 3, pp. 290–297, Mar. 2012, doi: 10.1016/j.chom.2012.01.016.

[80] T. Kuriakose *et al.*, "ZBP1/DAI is an innate sensor of influenza virus triggering the NLRP3 inflammasome and programmed cell death pathways," *Science Immunology*, vol. 1, no. 2, pp. aag2045–aag2045, Aug. 2016, doi: 10.1126/sciimmunol.aag2045.

[81] H. Koehler *et al.*, "Inhibition of DAI-dependent necroptosis by the Z-DNA binding domain of the vaccinia virus innate immune evasion protein, E3," *Proceedings of the National Academy of Sciences*, vol. 114, no. 43, pp. 11506–11511, 2017.

[82] R. J. Thapa *et al.*, "Interferon-induced RIP1/RIP3-mediated necrosis requires PKR and is licensed by FADD and caspases," *Proceedings of the National Academy of Sciences*, vol. 110, no. 33, pp. E3109–E3118, Aug. 2013, doi: 10.1073/pnas.1301218110.

[83] D. C. Chiang, Y. Li, and S. K. Ng, "The Role of the Z-DNA Binding Domain in Innate Immunity and Stress Granules," *Frontiers in Immunology*, vol. 11, 2021, Accessed: Aug. 30, 2022. [Online]. Available: https://www.frontiersin.org/articles/10.3389/fimmu.2020.625504

[84] H.-W. Chang, J. C. Watson, and B. L. Jacobs, "The E3L gene of vaccinia virus encodes an inhibitor of the interferon-induced, double-stranded RNA-dependent protein kinase," *Proceedings of the National Academy of Sciences*, vol. 89, no. 11, pp. 4825–4829, 1992.

[85] H.-W. Chang and B. L. Jacobs, "Identification of a conserved motif that is necessary for binding of the vaccinia virus E3L gene products to double-stranded RNA," *Virology*, vol. 194, no. 2, pp. 537–547, 1993.

[86] H.-W. Chang, L. H. Uribe, and B. L. Jacobs, "Rescue of vaccinia virus lacking the E3L gene by mutants of E3L.," *Journal of virology*, vol. 69, no. 10, pp. 6605–6608, 1995.

[87] H. Yuwen, J. H. Cox, J. W. Yewdell, J. R. Bennink, and B. Moss, "Nuclear localization of a double-stranded RNA-binding protein encoded by the vaccinia virus E3L gene," *Virology*, vol. 195, no. 2, pp. 732–744, 1993.

[88] J. C. Watson, H.-W. Chang, and B. L. Jacobs, "Characterization of a vaccinia virus-encoded double-stranded RNA-binding protein that may be involved in inhibition of the double-stranded RNA-dependent protein kinase," *Virology*, vol. 185, no. 1, pp. 206–216, 1991.

[89] T. A. Brandt and B. L. Jacobs, "Both carboxy-and amino-terminal domains of the vaccinia virus interferon resistance gene, E3L, are required for pathogenesis in a mouse model," *Journal of virology*, vol. 75, no. 2, pp. 850–856, 2001.

[90] W. D. Arndt *et al.*, "Evasion of the Innate Immune Type I Interferon System by Monkeypox Virus," *Journal of Virology*, vol. 89, no. 20, pp. 10489–10499, Oct. 2015, doi: 10.1128/JVI.00304-15.

[91] S. D. White and B. L. Jacobs, "The amino terminus of the vaccinia virus E3 protein is necessary to inhibit the interferon response," *Journal of virology*, vol. 86, no. 10, pp. 5895–5904, 2012.

[92] J. O. Langland and B. L. Jacobs, "Inhibition of PKR by vaccinia virus: role of the N-and C-terminal domains of E3L," *Virology*, vol. 324, no. 2, pp. 419–429, 2004.

[93] H. Koehler *et al.*, "Vaccinia virus E3 prevents sensing of Z-RNA to block ZBP1-dependent necroptosis," *Cell Host & Microbe*, vol. 29, no. 8, pp. 1266-1276.e5, Aug. 2021, doi: 10.1016/j.chom.2021.05.009.

[94] Z. Liu *et al.*, "A class of viral inducer of degradation of the necroptosis adaptor RIPK3 regulates virus-induced inflammation," *Immunity*, vol. 54, no. 2, pp. 247-258.e7, Feb. 2021, doi: 10.1016/j.immuni.2020.11.020.

[95] J. Z. Roberts *et al.*, "The SCFSkp2 ubiquitin ligase complex modulates TRAIL-R2-induced apoptosis by regulating FLIP(L)," *Cell Death Differ*, vol. 27, no. 9, pp. 2726–2741, Sep. 2020, doi: 10.1038/s41418-020-0539-7.

[96] J. Kindrachuk *et al.*, "Systems Kinomics Demonstrates Congo Basin Monkeypox Virus Infection Selectively Modulates Host Cell Signaling Responses as Compared to West African Monkeypox Virus *," *Molecular & Cellular Proteomics*, vol. 11, no. 6, Jun. 2012, doi: 10.1074/mcp.M111.015701.

[97] S. M. Cotsmire, M. Szczerba, and B. L. Jacobs, "Detecting Necroptosis in Virus-Infected Cells," in *Viruses as Therapeutics: Methods and Protocols*, A. R. Lucas, Ed. New York, NY: Springer US, 2021, pp. 199–216. doi: 10.1007/978-1-0716-1012-1_11.

[98] W. D. Arndt *et al.*, "Monkeypox virus induces the synthesis of less dsRNA than vaccinia virus, and is more resistant to the anti-poxvirus drug, IBT, than vaccinia virus," *Virology*, vol. 497, pp. 125–135, 2016.

[99] S. Nogusa *et al.*, “RIPK3 Activates Parallel Pathways of MLKL-Driven Necroptosis and FADD-Mediated Apoptosis to Protect against Influenza A Virus,” *Cell Host & Microbe*, vol. 20, no. 1, pp. 13–24, Jul. 2016, doi: 10.1016/j.chom.2016.05.011.

[100] B. P. Daniels *et al.*, “The Nucleotide Sensor ZBP1 and Kinase RIPK3 Induce the Enzyme IRG1 to Promote an Antiviral Metabolic State in Neurons,” *Immunity*, vol. 50, no. 1, pp. 64-76.e4, Jan. 2019, doi: 10.1016/j.immuni.2018.11.017.